

STEPHAN JUNG

Abiotic stress – A challenge for the master enzyme
plasma membrane H^+ -ATPase. A case study for
maize with special consideration of salt stress
and Mg deficiency



A thesis submitted for the requirement of the
doctoral degree in agricultural sciences
Faculty of Agricultural Sciences,
Nutritional Sciences, and Environmental Management
Justus Liebig University Giessen



edition mentalis
VVB LAUFERSWEILER VERLAG

Das Werk ist in allen seinen Teilen urheberrechtlich geschützt.

Die rechtliche Verantwortung für den gesamten Inhalt dieses Buches liegt ausschließlich bei dem Autor dieses Werkes.

Jede Verwertung ist ohne schriftliche Zustimmung des Autors oder des Verlages unzulässig. Das gilt insbesondere für Vervielfältigungen, Übersetzungen, Mikroverfilmungen und die Einspeicherung in und Verarbeitung durch elektronische Systeme.

1. Auflage 2017

All rights reserved. No part of this publication may be reproduced, stored in a retrieval system, or transmitted, in any form or by any means, electronic, mechanical, photocopying, recording, or otherwise, without the prior written permission of the Author or the Publishers.

1st Edition 2017

© 2017 by VVB LAUFERSWEILER VERLAG, Giessen
Printed in Germany



édition linguistique
VVB LAUFERSWEILER VERLAG

STAUENBERGRING 15, D-35396 GIESSEN
Tel: 0641-5599888 Fax: 0641-5599890
email: redaktion@doktorverlag.de

www.doktorverlag.de

Institute of Plant Nutrition
Justus Liebig University Giessen

Prof. Dr. Sven Schubert

**Abiotic stress – A challenge for the master enzyme plasma
membrane H⁺-ATPase. A case study for maize with special
consideration of salt stress and Mg deficiency**

**A thesis submitted for the requirement of the
doctoral degree in agricultural sciences
Faculty of Agricultural Sciences, Nutritional Sciences,
and Environmental Management
Justus Liebig University Giessen**

Submitted by

Stephan Jung

from Aachen

Giessen, September 2016

Date of thesis disputation: February 1, 2017

Examination Commission

Chairperson: Prof. Dr. Joachim Aurbacher

Supervisor: Prof. Dr. Sven Schubert

Co-supervisor: Prof. Dr. Sven Schubert

Examiner: Prof. Dr. Bernd Honermeier

Examiner: Prof. Dr. Rod Snowdon

To my parents

Table of contents

1. Introduction	1
1.1 Abiotic stress	1
1.2 Maize	2
1.3 Plasma membrane H⁺-ATPase	3
1.4 Mg deficiency	4
1.4.1 Mg – the forgotten macronutrient in crop production	4
1.4.2 Stumbling blocks for the determination of concentration in Mg-deficient plant material ..	9
1.5 Salt stress	11
1.6 Hypotheses	15
2. Materials and methods	17
2.1 Stumbling blocks for chlorophyll concentration measurements in Mg-deficient plant material	17
2.1.1 Plant cultivation and harvest	17
2.1.2 Pigment extraction	18
2.1.3 Determination of chlorophyll concentrations	18
2.1.4 Statistical analyses	19
2.2 Effect of Mg deficiency on plasma membrane H⁺-ATPase activity and the implications for maize growth	20
2.2.1 Plant cultivation and harvest	20
2.2.2 Analyses of cation, chlorophyll, sugar, and protein concentrations	21
2.2.3 Analyses of DNA content	22
2.2.4 Determination of apoplastic pH	22
2.2.5 Plasma membrane (PM) isolation	23
2.2.6 Kinetic assays of hydrolytic PM H⁺-ATPase activity	23
2.2.7 Measurement of proton-pumping activity	24
2.2.8 Relative abundance of RNA plasma membrane H⁺-ATPase isoforms	25
2.2.9 Gel electrophoresis and immune detection of plasma membrane H⁺-ATPases	27
2.2.10 Statistical analyses	27
2.3 Effect of salt stress on plasma membrane H⁺-ATPase activity and its implications for kernel development of maize	27
2.3.1 Plant cultivation and harvest	27
2.3.2 Sugar determination	29
2.3.3 Acid invertase enzyme extraction and activity measurements	30
2.3.4 Plasma membrane (PM) isolation of maize kernels	30

2.3.5 Kinetic assays of hydrolytic PM H ⁺ -ATPase activity of maize kernels	30
2.3.6 Measurement of proton-pumping activity of PM H ⁺ -ATPase of maize kernels	31
2.3.7 Relative abundance of RNA plasma membrane H ⁺ -ATPase isoforms.....	31
2.3.8 Gel electrophoresis and immunodetection of plasma membrane H ⁺ -ATPase	31
2.3.9 Statistical analyses	31
3. Results	33
3.1 Stumbling blocks for chlorophyll concentration measurements in Mg-deficient plant material	33
3.1.1 Effect of Mg deficiency on maize growth and N-tester results	33
3.1.2 Effect of addition of MgCO ₃ during extraction of maize leaves grown under Mg deficiency on chlorophyll concentrations	35
3.2 Effect of Mg deficiency on plasma membrane H ⁺ -ATPase activity and the implications for maize growth.....	37
3.2.1 Effect of slowly developing Mg deficiency on maize growth.....	37
3.2.2 Effect of Mg deficiency on chlorophyll, sugar, and protein concentrations of maize	39
3.2.3 Effect of Mg deficiency on DNA contents of maize	43
3.2.4 Effect of Mg deficiency on apoplastic pH of young developing leaves	45
3.2.5 Effect of Mg deficiency on plasma membrane H ⁺ -ATPase activity.....	46
3.3 Effect of salt stress on plasma membrane H ⁺ -ATPase activity and its implications for kernel development of maize	53
3.3.1 Effect of salt stress on maize yield determinants	53
3.3.2 Effect of salt stress on maize kernel sugar metabolism.....	57
3.3.3 Effect of salt stress on maize kernel PM H ⁺ -ATPase activity	61
4. Discussion	67
4.1 The photometric standard method using acetone extracts to determine chlorophyll is applicable to Mg-deficient maize tissue	67
4.2 Reduced assimilate availability in growing sink tissue is responsible for early growth inhibition under Mg deficiency in maize	70
4.3 Reduced cell division in growing sink tissue is responsible for early growth inhibition of maize under Mg deficiency	71
4.4 Altered PM H ⁺ -ATPase activity is responsible for reduced leaf apoplastic acidification reducing extension growth under Mg deficiency in maize.....	72
4.5 Source leaf sugar supply limits maize kernel development under salt stress	77
4.6 Sink hexose supply limits maize kernel development under salt stress	78
4.7 Plasma membrane H ⁺ -ATPase activity of young maize kernels is reduced under salt stress, inhibiting hexose uptake of the sink tissue, leading to kernel starvation	80
5. Conclusions.....	84

5.1	Reduced PM H⁺-ATPase activity limits cell-extension growth under Mg deficiency in maize.....	84
5.2	Reduced PM H⁺-ATPase activity limits maize kernel sugar uptake under salt stress	86
5.3	Contribution of the PM H⁺-ATPase to physiological responses under abiotic stress differs depending on plant organ	88
6.	Summary	90
7.	Zusammenfassung	92
8.	References	95
	Appendix	I
	Acknowledgment.....	IV
	Declaration.....	VII
	Curriculum Vitae	VIII

1. Introduction

1.1 Abiotic stress

The sessile nature of plants is a challenge: Abiotic stresses - arising from an excess or deficit in the physical or chemical environment - are threatening the plants' development on a regular basis. Examples for these physical or chemical constraints are: Nutrient excess or deficiency, heavy-metal toxicity, cold, heat, excess water, or water-limiting conditions. Even in agricultural systems, the total avoidance of abiotic stress is nearly impossible for plants. Consequently, crops rarely achieve their genetically predetermined maximum yield potential. Boyer (1982) estimated that field-grown crops in the United States just achieve 22% of their potential genetic yield due to abiotic stress. However, given the fact that plants face multiple situations with one or more abiotic stress events during their lifespan, plants have evolutionary determined strategies and mechanisms to cope with abiotic stresses. The extent to which a specific plant can cope with abiotic stress depends on the stress intensity, the plant's individual evolutionary set of available strategies, and their underlying mechanisms to counter the stress impact. These sets of countermeasures are species or even genotype- specific. However, some strategies can be found in nearly all land plants, e.g. the strategy to accumulate osmotically active solutes under drought stress in order to decrease the osmotic potential in cells to ensure water uptake by roots. Many others strategies and especially their underlying mechanisms are often very specific among plant species. Mostly they are still unknown even for important agricultural crop plants. Understanding of these strategies and mechanisms is imperative in order to use this knowledge to increase yield security in the plant breeding process (Cramer et al., 2011). Improving crops by plant breeding is the only viable way, since crop plants are of a sessile nature, and the extent to which plant production systems can reduce abiotic stresses

is limited. This is especially true for the most important crop plants on which world food security depends on.

1.2 Maize

Maize is one of the world's most important crop plants. It is the second largest agricultural commodity in terms of tons, stressing its worldwide importance. The world production of the commodity maize increased from roughly 600 million tons in the year 2000 to over 1 billion in 2014 which means a yearly growth rate of 4% (FAO, 2015).

Maize or corn (*Zea mays* L.) belongs to the family *Poaceae* together with its ancestor the wild plant teosinte. Its origin is the region of Mesoamerica where the C₄ plant was domesticated by selection of key mutations (Matsuoka et al., 2002). The grains are used for human and livestock consumption as well as for the ethanol production; therefore, total grain yield is an important agronomical factor. There are two components of grain yield: Kernel number and kernel weight. Both components can be negatively affected by abiotic stress. However, a lower kernel number is often partly compensated by a higher grain weight, depending on stress intensity and the physiological stage in which the stress occurs (Borrás et al., 2003). There is apparently an evolutionary-conserved strategy to maintain the full kernel set. Schubert et al. (2009) developed salt-resistant maize hybrids which are able to maintain kernel set under salt stress. In contrast, kernel setting of salt-sensitive genotypes is affected by salt stress. This example shows that maize has an unexplored genetic potential to implement strategies in future breeding processes which could prevent the reduction of yield due to abiotic stress. These strategies and their underlying mechanisms have to be identified and understood in order to use this knowledge in plant breeding programs.

1.3 Plasma membrane H⁺-ATPase

The plasma membrane (PM) H⁺-ATPase is the powerhouse of the plant metabolism, since it is responsible for the energization of most transport processes in plants. The energization is conducted by the establishment of an electrochemical proton gradient across the plasma membrane (Palmgren, 2001). The active transport of protons is fueled with the substrate Mg-ATP (Hanstein et al., 2011). The proton transport into the apoplasmic space acidifies the cell wall. This acidification of the cell wall is a requisite for cell-extension growth (Hager et al., 1971; Dünser and Kleine-Vehn, 2015). Additionally, cations cross the plasma membrane through ion channels, attracted by the negative membrane potential of the cytoplasm. The electrochemical gradient energizes transport processes of symporters and antiporters in the PM (Palmgren, 2001).

Since the PM H⁺-ATPase is so important for plant physiological processes, it is not astonishing that abiotic stress has an impact on the function of the enzyme (Palmgren, 1991; Falhof et al., 2016). The enzyme has an auto-inhibitory domain at the C-terminus. Binding of effector molecules or phosphorylation at the auto-inhibitory domain has a strong influence on the enzymes activity. There are two activity states: an auto-inhibited state, where ATP hydrolysis is only loosely coupled to H⁺ transport, and an upregulated state with tight coupling between ATP hydrolysis and H⁺ pumping (Falhof et al., 2016). There are various phosphorylation sites at the auto-inhibitory domain that can be affected either by phosphorylation or dephosphorylation reactions caused by various environmental stimuli including abiotic stress. This flexibility of the enzyme regarding the H⁺ pumping activity can be used for breeding strategies. Therefore, alteration of the PM H⁺-ATPase activity can play an important role in strengthening mechanisms that help to counteract abiotic stress.

For example, Gévaudant et al. (2007) showed that salt resistance of tobacco was improved since one isoform of PM H⁺-ATPase was constitutively activated and expressed in transgenic tobacco. It was confirmed that these transformed plants were able to increase the pH gradient at the plasma membrane of root cells. The electrochemical gradient that is generated by the PM H⁺-ATPase energizes the SOS1 Na⁺/H⁺ antiporter. It is believed that the higher pH gradient increased the pumping activity of SOS1, which excluded potential toxic Na⁺ from the cytoplasm and increased growth of the transformed tobacco compared to the wildtype under salt stress. There are other examples: It was also shown that the maize hybrid Pioneer 3906 was not able to maintain apoplastic acidification in developing leaves under salt stress, which resulted in a reduction of turgor-driven cell-extension growth. In contrast, a salt-resistant maize genotype (SR03) that was bred from the same genetic background as Pioneer 3906 was able to maintain or even to increase the apoplastic acidification and to decrease growth reduction under salt stress (Zörb et al., 2015). Thus, the genetic potential to reduce the impacts of salt stress on growth by improving the pumping activity of PM H⁺-ATPase had already been available and was brought into light in a newly bred hybrid.

1.4 Mg deficiency

1.4.1 Mg – the forgotten macronutrient in crop production

Mg is one of the nine macronutrients for plants and a deficiency in only one plant nutrient unavoidably leads to a disturbed plant development and a consequent yield loss. Astonishingly, magnesium (Mg) is often neglected in the agricultural fertilization practice (Guo et al., 2016). The negligence of Mg fertilization is responsible for crop yield losses worldwide caused by Mg deficiency in plants.

In plants, Mg plays an important role in the structure of chlorophyll, the assembly of ribosome subunits during translation, and the activation of various enzymes (Shaul, 2002; Hawkesford et al., 2012). Moreover, Mg is essential for the formation of Mg-ATP which is the true substrate for the plant PM H⁺-ATPases (Palmgren, 2001; Hanstein et al., 2011). In recent years, studies on Mg transporters and their efficiency under low Mg conditions were conducted (Hermans et al., 2013; Kobayashi and Tanoi, 2015), increasing the knowledge about Mg uptake by plants considerably. However, little is known about the physiological processes which are impaired under Mg deficiency and inhibit plant growth. Particularly, it is important to know which physiological process is most sensitive to a developing Mg deficiency and is responsible for impaired vegetative growth. (Cakmak et al., 1994a) described that one of the first processes affected under Mg deficiency was the translocation of sucrose from source leaves to roots. It was concluded that a lack of assimilates led to growth inhibition of roots, since roots as a sink organs are like developing young leaves dependent on assimilates from source tissue: Photosynthetic active leaves. An accumulation of sugars in source leaves was also found in other plant species due to Mg deficiency: Bean plants (Cakmak et al., 1994a), maize (Mengutay et al., 2013), spinach (Fischer et al., 1998), and sugar beet (Hermans et al., 2004a).

Some authors supposed that a decrease of PM H⁺-ATPase activity was responsible for a reduced phloem transport of sucrose from leaf source tissue to sink tissues (e.g. (Cakmak et al., 1994a; Neuhaus et al., 2013). Since sucrose is mostly loaded into the phloem by sucrose/ H⁺ cotransporters, a decrease in the substrate Mg-ATP for the PM H⁺-ATPase undoubtedly leads to a lower pH gradient which in turn reduces the transport rate of sucrose as well. However, even if PM H⁺-ATPase activity is partially impaired under Mg deficiency (which was never measured), the

question remains whether a reduced loading of photoassimilates into the phloem in source leaves would also mean that there is a lack of photoassimilates in the sink tissue that reduces plant growth.

For example, Hermans and Verbruggen (2005) using radiolabeled sucrose, showed that sucrose transport from the source leaves of *Arabidopsis* to the roots was not inhibited. Fischer et al. (1998) found for spinach that sugars also accumulated in sink leaves that were shaded. This shading prevented photosynthetic activity of these sink leaves, making the sink leaves entirely dependent on photoassimilates from source leaves. From these findings, it can be concluded that apparently photosynthesis is not the primary limiting process of plant growth under Mg-limiting conditions.

However, since growth of sink organs such as roots or developing leaves is impaired by Mg deficiency, there have to be other reasons. To our knowledge no study has been conducted which considered the effect of Mg deficiency on the two growth processes cell division and cell extension separately. In order to identify the process that is most sensitive to Mg deficiency, these growth processes cell division and cell extension were studied in the present work including their underlying physiological mechanisms.

Both, DNA replication and gene expression determine the rate of cell division. The Mg concentration in the cytoplasm has to be in an optimal range for both processes for normal function (Stout and Arens, 1970; Robinson and Bryant, 1975; Kiss, 1988). Therefore, if a lack of Mg inhibits the DNA polymerase activity, a lower number of DNA will be present in the analyzed tissue. Since DNA replication is required for cell division, a lower DNA content indicates a lower number of cells. The proportion of mitochondrial and chloroplast DNA of maize just account for about 0.4%

of the total cell DNA and is therefore negligible (Lutz et al., 2011). Additionally, cell division in maize just occurs in a thin cell layer close to the apex (Jackson, 2009). Above this thin cell layer, the meristematic tissue, cell growth is only realized by cell-extension growth in maize.

Cell-extension growth is driven by apoplastic acidification that is necessary for the loosening of cell-wall compounds, which in turn enables turgor-driven extension growth (Figure 1). Plasma membrane (PM) H⁺-ATPases play an important role in cell-extension growth, because these enzymes are responsible for cell-wall acidification (Bogoslavsky and Neumann, 1998; Waldron and Brett, 2008; Pitann et al., 2009; Dünser and Kleine-Vehn, 2015).

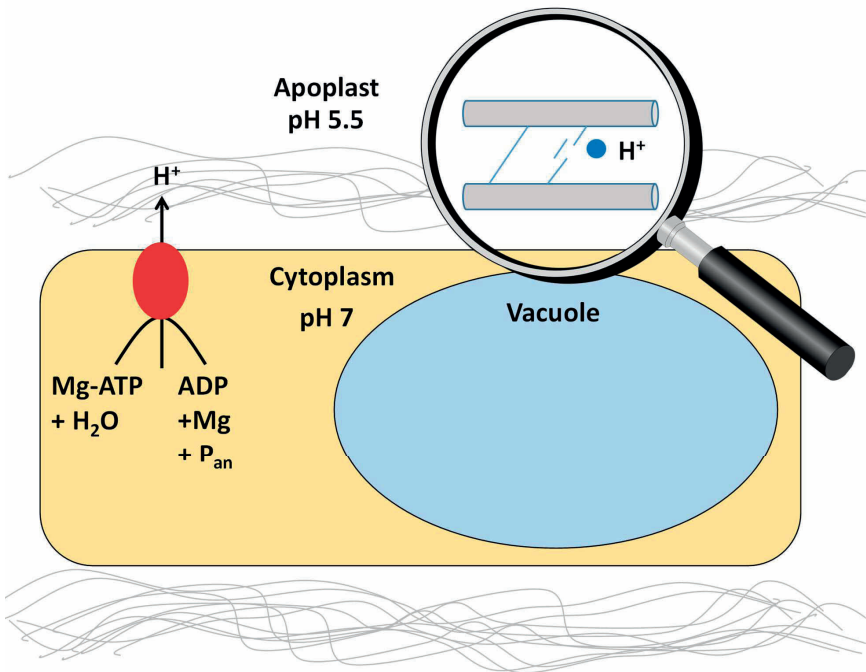


Figure 1: Apoplastic acidification is mainly driven by plasma membrane (PM) H⁺-ATPase (red oval). Cell wall loosening enzymes (blue circles) are activated by low pH, breaking connections between polysaccharide chains such as pectin, cellulose, and hemicellulose (grey lines). Turgor facilitates cell-extension growth. (inspired by Dünser and Kleine-Vehn, 2015)

In order to identify the limiting process for vegetative growth of maize under Mg deficiency, time-course experiments with maize were conducted under control and Mg-deficient conditions to identify which physiological process is most sensitive to Mg deficiency. It was tested whether assimilate availability and/ or cell division in sink tissue limits growth. In addition, it is hypothesized that a reduced apoplastic acidification limits extension growth by decreased PM H⁺-

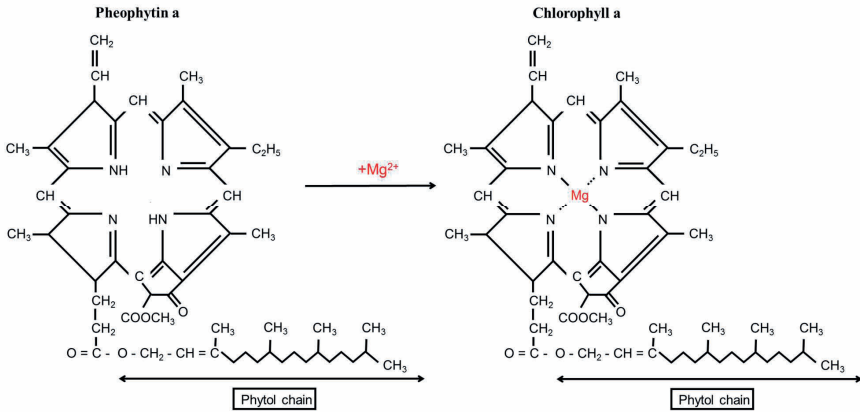
ATPase activity and that the expression pattern of H⁺-ATPase isoform transcripts is altered under Mg deficiency.

1.4.2 Stumbling blocks for the determination of concentration in Mg deficient plant material

Approximately 10% of Mg in plants are bound as central atom of chlorophyll and a reduction in chlorophyll concentration is often found under Mg deficiency (Hawkesford et al., 2012). However, some studies showed that the chlorophyll concentrations under Mg deficiency were affected a few days after plant growth and other physiological parameters (Hermans et al., 2004b; Cakmak and Kirkby, 2008). It is astonishing that other physiological processes are impaired when such a big share of the plants' total Mg content is used for chlorophyll. Therefore, it was questioned whether the standard method for chlorophyll determination in leaves is suitable for leaf tissue that was cultivated under Mg-deficient conditions.

A standard method for chlorophyll determination is the extraction of pigments with organic solvents such as acetone, ethanol or methanol and the following quantification. Before extraction, MgCO₃ is often added to the leaf tissue in order to avoid the loss of Mg as central atom of chlorophyll during the extraction process (Wrolstad et al., 2004; Zörb, 2004). However, Mg could be inserted non-enzymatically or enzymatically into Mg-free chlorophyll precursors or metabolites during pigment extraction of leaf tissue with organic solvents (Figure 2). This could lead to an overestimation of chlorophyll concentrations, especially in plants grown under Mg-deficient conditions. Highly concentrated organic solvents do not guarantee a total inhibition of enzymes. Hu et al. (2013) showed that chlorophyll was converted to chlorophyllide during pigment extraction

with organic solvents, because the ester bond of chlorophyll was hydrolyzed by means of the still active enzyme chlorophyllase (EC: 3.1.1.14), resulting in chlorophyllide and a phytol chain.



2+

Figure 2: Theoretical transformation of pheophytin a into chlorophyll a by addition of Mg²⁺ as MgCO₃ or other Mg salts. Other pheopigments such as protoporphyrin IX may also be susceptible.

One goal of this study was to investigate the effect of MgCO₃ addition before extraction of plant pigments on chlorophyll concentrations, in order to evaluate the conventional photometric chlorophyll determination procedure in maize leaves grown under Mg deficiency. Consequently, it is hypothesized that the Mg chelatase (EC: 6.6.1.1) is still active in an aqueous acetone extract and inserts free Mg, added as MgCO₃ prior extraction, into protoporphyrin IX or other Mg-free porphyrin molecules, especially in plant tissue grown under Mg-deficient conditions. As a reference method, the non-destructive chlorophyll determination with the N-tester was used.

1.5 Salt stress

Salinity is one of the major reasons for yield losses of crops in areas where evapotranspiration exceeds precipitation. This natural occurrence is worsened by irrigation practices that are not adapted to the environmental conditions in arid and semiarid areas (Qadir et al., 2006). Besides increasing efforts to avoid anthropogenic salinization of soils and active attempts of soil desalinization salt-resistant crops are grown to diminish salt stress effects. In order to develop those crops the physiological processes which lead to yield losses under salt stress have to be understood (Munns, 2011).

A model explaining the main physiological effects of salt stress on wheat was first developed by Munns (1993) and refined by Munns and Tester (2008). The model describes two phases of salt stress that affect wheat growth. The model was confirmed for maize by Schubert (2011) and extended to an additional phase (Figure 3). Phase 0 occurs directly after initializing salt stress, affecting plants' water uptake and causing a strong decrease of growth. Phase 0 is followed by Phase I that exhibits a recovery of growth rate which is however still lower than under unstressed conditions. This osmotic phase is similar to drought stress (Munns, 2011). Phase II is entered when salt concentrations reach toxic levels in plant tissues. In maize, Na^+ accumulates especially in older leaves, causing necrosis of leaf tissue (Fortmeier and Schubert, 1995). The described effects mainly occur in the vegetative growth stage. However, they have also consequences for the generative growth stage.

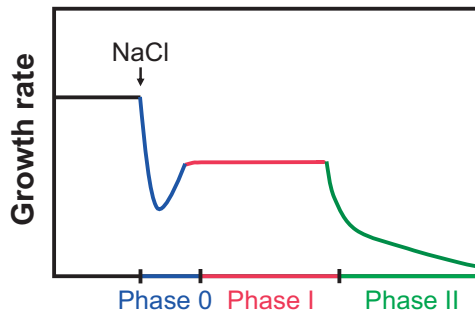


Figure 3: Model of three-phase growth reduction of maize by salt stress (Schubert 2011).

It is well known that abiotic stress such as salt stress reduces the number of maize kernels reaching maturity (Schubert et al., 2009; Hütsch et al., 2015). Earlier studies found that a reduction in kernel number is caused by decreased sugar availability in the maize kernels if drought stress occurs in the weeks around husk emergence and right after silk pollination (Zinselmeier et al., 1999). The authors concluded that the assimilate supply to the kernels was reduced due to the decrease of acid invertase activity under drought stress. More recently, Oury et al. (2015) and Oury et al. (2016) showed that maize silk development was impaired by drought stress, leading to a reduced fertilization of ovaries and thus to less kernels, especially in the apical part of maize cobs. In these drought-stress studies, acid invertase activity was reduced. However, not only sucrose accumulated in kernel tissue, but also hexose concentrations were higher or at least not reduced under drought stress. Therefore, the authors argued that not a lack of hexoses led to kernel abortion, but rather a reduction in successful ovary fertilization.

In our previous study we also found that a reduction of acid invertase activity around pollination occurred under drought stress as well as under salt stress (Hütsch et al., 2015). Additionally, we showed that while acid invertase activity was strongly reduced, the hexose concentrations were not. Instead, they were even higher under both stress conditions. While a higher sucrose concentration is a good parameter to exclude that source limitation is responsible for kernel starvation and abortion (Henry et al., 2015; Hütsch et al., 2015; Oury et al., 2016), higher hexose concentrations do not necessarily rule out kernel starvation. On the opposite, higher hexose concentrations could very well point to kernel starvation and subsequent abortion. The maternal and daughter cell tissues of the kernels are physically isolated from each other due to a lack of plasmodesmata (symplastic) continuity (Tang and Boyer, 2013). Therefore, after unloading of sucrose from phloem, driven by acid invertase activity, the resulting hexoses have to be transported from the apoplast of pedicle and placento-chalaza tissue into the cytoplasm of the endosperm tissue by hexose carriers (Bihmidine et al., 2013). These carriers are hexose/ H^+ symporters which are energized by the pH gradient at the plasma membrane (Figure 4). This pH gradient is established by the PM H^+ -ATPase (Sondergaard et al., 2004).

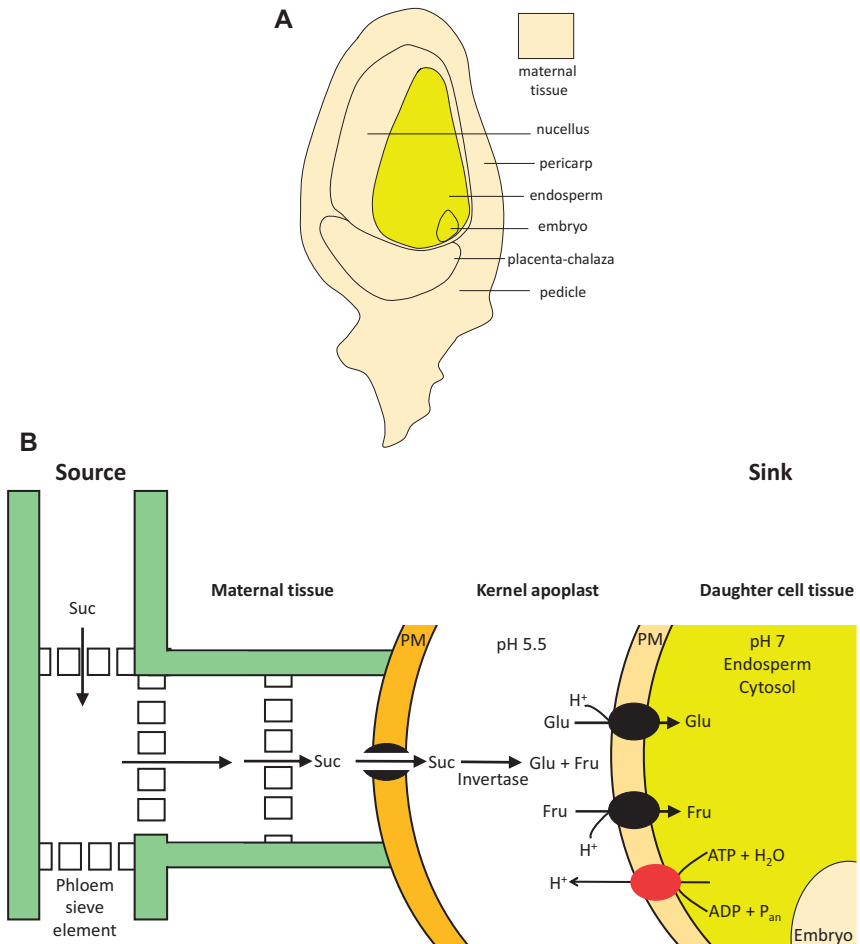


Figure 4: (A) Morphology of young maize kernels (redrawn after Bihmidine et al., 2013). (B) Sucrose (Suc) transport from source (leaves) to the sink (kernels) of maize. Suc moves through the phloem to the sink where it is released non-selectively through the plasma membrane (orange). In the kernels apoplast it is hydrolyzed by means of acid invertase to Glucose (Glu) and Fructose (Fru). The daughter cells take up Glu and Fru selectively with hexose transporters (black). The transporters are energized with the pH gradient, established by the PM H^+ -ATPase (red). (Partly redrawn after Tang and Boyer, 2013).

Under salt stress, the activity of this enzyme is often reduced in maize leaves during the vegetative stage (Zörb et al., 2005b; Hatzig et al., 2010). If the activity of the PM H⁺-ATPase is also reduced in the developing maize kernels under salt stress, the pH gradient will not be properly established, resulting in an accumulation of hexoses in the apoplast. Reduced transport of hexoses into the cytoplasm could then lead to kernel starvation in the first days after fertilization. No other studies are known which investigated the relationship between PM H⁺-ATPase activity and kernel abortion. Therefore, it was hypothesized that kernel PM H⁺-ATPase activity is inhibited by salt stress, resulting in reduced hexose uptake which in turn leads to kernel abortion.

1.6 Hypotheses

In the first part of this thesis the effect of the abiotic stress Mg deficiency on the PM H⁺-ATPases' and their involvement in the vegetative growth process of maize were examined. In addition, other physiological parameters which are not directly dependent on the PM H⁺-ATPase were also investigated in order to determine their contribution to reduced vegetative growth under Mg deficiency. A standard method for chlorophyll determination was examined to evaluate if it is applicable for Mg-deficient plant material. Therefore, the following hypotheses were tested:

- 1. The photometric standard method using acetone extracts to determine chlorophyll concentrations is applicable to Mg-deficient maize tissue.*
- 2. Reduced assimilate availability in growing sink tissue is responsible for early growth inhibition under Mg deficiency in maize.*

3. Reduced cell division in growing sink tissue is responsible for early growth inhibition of maize under Mg deficiency.

4. Altered PM H⁺-ATPase activity is responsible for reduced leaf apoplastic acidification reducing extension growth under Mg deficiency in maize.

In the second part of this thesis the effect of the abiotic stress salinity on the PM H⁺-ATPases and their role in the generative stage, namely in the development of young maize kernels and grain yield were examined by testing the following hypotheses:

5. Source leaf sugar supply limits maize kernel development under salt stress.

6. Sink hexose supply limits maize kernel development under salt stress.

7. Plasma membrane H⁺-ATPase activity of young maize kernels is reduced under salt stress, inhibiting hexose uptake of the sink tissue, leading to kernel starvation.

2. Materials and methods

2.1 Stumbling blocks for chlorophyll concentration measurements in Mg-deficient plant material

2.1.1 Plant cultivation and harvest

The experiment was set up in hydroponics in a completely randomized design with four replications and two Mg treatments: Mg control (500 μM) and Mg deficiency (25 μM). Maize seeds (*Zea mays* L. cv. Amadeo) were soaked in aerated 1 mM CaSO_4 solution for 1 d and then packed between filter paper moistened with 1 mM CaSO_4 . The seeds germinated in the dark for 3 d and in the light for 4 d. The experiment was conducted in a climate chamber under the following conditions: light intensity was 500 $\mu\text{E m}^{-2} \text{s}^{-1}$ (Philips Master HPI-T Plus 400 W) for 16 h at 26°C and 18°C for 8 h in the dark period, respectively. The relative humidity was 50%. On day 8, plants were transferred into plastic pots (eight plants per pot) containing 10 L of aerated half-strength nutrient solution. The plants received full-strength nutrient solution on day 12 (4 d after start of differential Mg treatment). The full-strength nutrient solution for control plants contained (in mM): $\text{Ca}(\text{NO}_3)_2$, 2.0; K_2SO_4 , 1.0; KH_2PO_4 , 0.2; MgSO_4 , 0.5; CaCl_2 , 2.0; Na_2SiO_3 , 1.0 (in μM) H_3BO_4 , 1.0; MnSO_4 , 2.0; ZnSO_4 , 0.5; CuSO_4 , 0.3; $(\text{NH}_4)_6\text{Mo}_7\text{O}_{24}$, 0.01; Fe-EDTA, 200; NiSO_4 , 0.1. In the Mg-deficiency treatment (25 μM Mg), 475 μM CaSO_4 were used to supplement the missing S. Plants were harvested 5 d and 8 d after onset (DAO) of differential Mg treatment. Before each harvest, the light transmission was measured individually for each investigated leaf (30 measurements leaf⁻¹ pot⁻¹) with a chlorophyll meter (N-tester[®], Yara International ASA, Oslo). Fresh weight was determined separately for each leaf and plant material was immediately frozen in liquid N_2 . Plant material was

ground with mortar and pestle in liquid N₂ and stored at -20°C until further analysis. Part of the ground plant material was lyophilized for dry-weight determination.

2.1.2 Pigment extraction

Chlorophyll concentration was determined after aqueous acetone extraction (Zörb, 2004). Frozen plant material (0.8 or 1.0 g) was extracted with acetone. The final acetone concentration was 80%; the individual water contents of the different leaves were considered to adjust the target acetone concentration. Each biological replicate was extracted twice: with and without MgCO₃ addition (50 mg) to the frozen plant material before extraction with acetone. The samples were kept in the dark and on ice before and after extraction until spectrophotometric measurement at 5°C.

2.1.3 Determination of chlorophyll concentrations

Chlorophyll a and b concentrations were measured photometrically at 664 nm and 647 nm in quartz cuvettes (Cary 100, Agilent). In addition, an absorption spectrum for each sample was recorded ranging from 350 to 900 nm. The concentrations were calculated by means of the equations given by Porra et al. (1989):

$$\text{Chlorophyll a conc. } (\mu\text{g mL}^{-1}) = 12.25 A_{664} - 2.55 A_{647}, \quad (1)$$

$$\text{Chlorophyll b conc. } (\mu\text{g mL}^{-1}) = 20.31 A_{647} - 4.9 A_{664}, \quad (2)$$

$$\text{Chlorophyll a+b conc. } (\mu\text{g mL}^{-1}) = 17.76 A_{647} + 7.34 A_{664}. \quad (3)$$

In order to investigate the possibility of subliminal enzymatic or non-enzymatic reactions in the filtered leaf-acetone extract, the extracts were also incubated at 25°C for 10 min and the light absorbance was measured afterwards as described above. In addition to the normal extraction method, a modified extraction method was used. The plant material was incubated with deionized water (with and without 50 mg MgCO₃) at 25°C for 10 min before acetone extraction. This was done to exclude the possibility that protoporphyrin IX or other Mg-free porphyrine molecules, already existent in plant leaves and especially in plant tissues grown under Mg deficiency, were converted to chlorophyll during the extraction process. To quantify the pheophytin concentrations in the pigment extracts, each plant acetone-extract was acidified immediately after photometrical measurement by the addition of 10 µL 8 M HCl (3 mL chlorophyll extract), which resulted in a pH in the range of 2.0-2.5. Chlorophyll was transformed to pheophytin by HCl addition and the extracts were measured again at 665 nm to calculate the pheophytin concentrations. The pheophytin concentrations were calculated by means of the equation given by Lorenzen (1967):

$$\text{Pheophytin a conc. } (\mu\text{g mL}^{-1}) = 26.7 [1.7 A_{665} (\text{after acidification}) - A_{664} (\text{before acidification})], \quad (4)$$

2.1.4 Statistical analyses

Data shown are means of four biological replications. Variations among biological replications are characterized by standard errors (\pm SE). Control and Mg-deficient treatments were compared using the two-tailed student's t-test. Likewise, the samples augmented with MgCO₃ were compared to the samples without MgCO₃ addition by means of the two-tailed student's t-test.

2.2 Effect of Mg deficiency on plasma membrane H⁺-ATPase activity and the implications for maize growth

2.2.1 Plant cultivation and harvest

In order to identify the most sensitive physiological process under Mg deficiency several parameters were measured. For these measurements a sufficiently large amount of plant material was needed, making several experiments necessary. All experiments were conducted under the same experimental conditions. The first experiment was conducted to determine the time frame in which growth reduction occurred after onset of Mg deficiency, as well as for the determination of DNA content and concentrations of sugars, chlorophyll, and protein. The second experiment was conducted to determine the effect of Mg deficiency on the apoplastic pH of developing leaves. The third experiment was conducted to confirm the results of Experiment 2 and to measure the relative RNA abundance of different H⁺-ATPase isoforms. The last experiment was conducted to isolate plasma membrane vesicles for the determination of hydrolytic and pumping activity of PM H⁺-ATPases.

The experiments were set up in a completely randomized design in hydroponics with four replications and two Mg treatments: Mg control (500 μM) and Mg deficiency (25 μM). Maize seeds (*Zea mays* L. cv. Amadeo) were soaked in an aerated 1 mM CaSO₄ solution for 1 d and then packed between filter paper moistened with 1 mM CaSO₄. The seeds were germinated for 3 d in the dark and 4 d in the light. Plants were grown in a climate chamber at 26°C for 16 h light period (light intensity was 500 μE m⁻² s⁻¹) and at 18°C for 8 h dark period. The relative humidity was 50%. On day 8, 70 plants were transferred into boxes containing 40 L of aerated half-strength nutrient solution (eight boxes control, eight boxes Mg deficiency). At this time, the different Mg

treatments were started. Plants received full-strength nutrient solution 1 d after the onset (DAO) of differential Mg nutrition. The control full-strength nutrient solution contained (in mM): $\text{Ca}(\text{NO}_3)_2$, 1.0; NH_4NO_3 1.0 K_2SO_4 , 1.0; KH_2PO_4 , 0.2; MgSO_4 , 0.5; CaCl_2 , 2.0; Na_2SiO_3 1.0; (in μM) Fe-EDTA, 200; H_3BO_3 , 1.0; MnSO_4 , 2.0; ZnSO_4 , 0.5; CuSO_4 , 0.3; $(\text{NH}_4)_6\text{Mo}_7\text{O}_{24}$, 0.01; NiSO_4 , 0.1. In the Mg deficiency treatment (25 μM Mg), 475 μM CaSO_4 were used to supplement the missing S. In order to obtain a time course of emerging Mg deficiency, plants were harvested every day or every second day. The nutrient solution was renewed every second day. In the morning of each day, the widths and lengths of individual leaf blades were measured. Leaf blade area was calculated as the product of width and length divided by 2. The plant organs (shoots and roots) were pooled. Shoots were divided into separate leaves; leaves 1 and 2 were preserved together. Fresh weights were determined for every individual plant part and plant material was frozen immediately in liquid N_2 . Roots were sopped in 1 mM CaSO_4 solution, washed with deionized water and blotted dry with paper towels before fresh-weight determination. Plant material was ground with mortar and pestle in liquid N_2 for further analyses and stored at -80°C . A part of the ground plant material was lyophilized for the determination of soluble sugars. An aliquot of the plant material was oven-dried at 105°C for cation determination.

2.2.2 Analyses of cation, chlorophyll, sugar, and protein concentrations

Cations were analyzed after dry-ashing of the plant material at 550°C . The ash was boiled with 5 mL 5 M HNO_3 and, after filtration, cation concentrations were measured with AAS (Varian Spectra AA 220FS). Pigments were extracted with aqueous acetone (80%) from the frozen plant material, in the presence of MgCO_3 . The chlorophyll a+b concentrations were measured according to Zörb (2004). The sugars glucose, fructose, and sucrose were determined enzymatically with UV

test kits (Boehringer Mannheim/Roche-Biopharm). Approximately 10 mg of lyophilized plant material were extracted in 75°C hot deionized water for 30 min. After centrifugation, the extracts were analyzed according to the manufacturer's instructions and measured photometrically at 340 nm. Protein concentrations were determined with the Bradford method (Bradford, 1976) after extraction of 100 mg lyophilized plant material with phosphate-buffered saline Tween (PBST).

2.2.3 Analyses of DNA content

DNA was isolated from frozen plant material (100 mg) using the Qiagen®DNeasy Plant Mini Kit according to the manufacturer's instructions. DNA concentration was determined photometrically (Varian Cary 4 Bio) with a TrayCell (Model 105.810-UVS by Hellma) at 260 nm and purity was determined as the 280 nm : 260 nm ratio. DNA content was calculated by multiplication of DNA concentrations and leaf or root dry weight.

2.2.4 Determination of apoplastic pH

In Experiments 2 and 3, leaf-blade tissue of 3 cm² of the growing zone of developing leaves was excised with a razor blade. The apoplast of leaf segments was infiltrated with 50 mM fluorescein isothiocyanate (FITC)-dextran (MW = 10,000 g mol⁻¹, Sigma-Aldrich, Germany) by means of the vacuum-infiltration technique (Mühling and Läubli, 2000). The apoplastic pH was calculated after measuring the fluorescence-emission intensity of several spots of each leaf blade (Pitann et al., 2009).

2.2.5 Plasma membrane (PM) isolation

Plasma membrane vesicles were isolated from the growing 4th leaf blade 5 d after onset of differential Mg nutrition. The lower part of this leaf blade, which was still partly covered with the surrounding 3rd leaf, was used for vesicle isolation. This leaf part was chosen to obtain still expanding leaf tissue. The plant material was placed on ice immediately after cutting. The material was homogenized according to Briskin and Poole (1983), De Michelis and Spanswick (1986), and Galtier et al. (1988). Phase partitioning of membranes was performed with a polymer concentration of 6.2% (Zörb et al., 2005a; Hanstein et al., 2011). Quantification of proteins was done with the method of Bradford (1976). Vesicle aliquots were stored in liquid N₂. Vesicle purity was confirmed using specific ATPase and pyrophosphatase inhibitors (Gallagher and Leonard, 1982; Yan et al., 1998; Hanstein et al., 2011).

2.2.6 Kinetic assays of hydrolytic PM H⁺-ATPase activity

In order to determine the Michaelis constant (K_m) and turnover number (K_r) of the PM H⁺-ATPase (EC: 3.6.3.6) the hydrolytic activity of each sample was measured for ten different ATP concentrations in each assay. The hydrolytic activity assays were conducted in the presence of either 5 or 1 mM Mg according to Hanstein et al. (2011). The Michaelis constant (K_m) is the substrate concentration at which the reaction rate is half of V_{max} , which represents the maximum reaction rate achieved by an enzyme at maximum substrate saturation. The turnover number (K_r) is defined as the maximum number of chemical conversions of substrate molecules per second that a single catalytic site executes for a given enzyme concentration. It is calculated by dividing V_{max} by the catalyst site concentration $[E]_T$.

Normalization of ATPase activities

The normalization procedure eliminated slight variations in enzyme concentrations of replicates. Such differences could have occurred when enzyme concentrations slightly differed between stored vesicle aliquots for replicates. Normalized activities were determined for each replicate as follows: (i) calculating the sum of activities over the whole range of ATP concentrations for each replicate (individual sum), (ii) determining the mean sum of all replicates, and (iii) multiplying the activity values of a replicate with the ratio between the mean sum and the individual sum of that replicate (Hanstein et al. 2011).

Non-linear regression analysis with DynaFit

The measured activity data were subjected to non-linear regression analysis as described by (Hanstein et al., 2011). DynaFit was used to fit a mechanistic model to the measured enzyme activities (Kuzmič, 1996). All calculations were based on the measured activities of four biological replicates. In all fitting procedures, the rate constants for association were used as constants (based on literature values), and the rate constants for dissociation were used for fitting. The fitting procedure requires that initial values are specified which were also derived from literature values (Wang et al., 2013). All constants and initial values are defined in the used DynaFit script (Appendix Figure 1).

2.2.7 Measurement of proton-pumping activity

The formation of a pH gradient across the plasma membrane of inside-out vesicles was measured as the quenching of absorbance by acridine orange (AO) at 492 nm (ΔA_{492}) at a Mg concentration

of 5 mM (Yan et al., 1998) (Figure 5). Proton transport was characterized using the following parameters: Active transport was quantified as initial rate during the first 2 min after addition of Mg-ATP. The maximum pH gradient was determined as the maximum quenching of absorbance (ΔA_{492}), and passive proton transport was determined as initial rate of proton efflux for 1 min after addition of the specific inhibitor of PM ATPase vanadate.

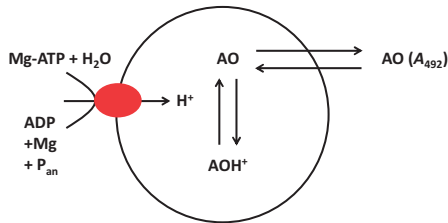


Figure 5: Determination of the pH gradient across the plasma membrane of inside-out vesicles, measured as the quenching of absorbance by acridine orange (AO).

2.2.8 Relative abundance of RNA plasma membrane H⁺-ATPase isoforms

In silico analysis of the maize genome (<http://www.maizegdb.org/>; Maize B73 RefGen_v2) allowed the identification of ten candidate genes for PM H⁺-ATPase isoforms. However, only six of the candidates were reported to be transcribed in leaf tissue (Sekhon et al., 2011). These six leaf isoforms of PM H⁺-ATPase were defined as MHA1-6 in the present study. The stability of transcription level of six reference genes, which were suggested by Manoli et al. (2012), were tested in the selected leaf segments. Cullin (CUL) and ubiquitin carrier protein (UBCP) were assessed as most stable reference genes using the algorithm of the Normfinder software (<http://moma.dk/normfinder-software>) and were used as normalization base for the present experiment. Primer pairs representing six different PM H⁺-ATPase isoform genes were designed

using Primer3Plus (ver. 0.4.0; <http://frodo.wi.mit.edu/primer3>) and the PRaTo software (<http://prato.daapv.unipd.it/>) was used to rank the primer pairs according to their qPCR performing potential (Nonis et al. 2011). To increase the specificity of amplification primers were designed in the 3' UTR region of the genes and were tested *in silico* for specificity by means of NCBI primer blast (<http://www.ncbi.nlm.nih.gov/tools/primer-blast/>). Accession number, primer sequence, their position on transcript, and expected size of amplicon are provided in Appendix Table 1.

Approximately 100 mg frozen plant material derived from the same growing leaf blade segments as for the apoplastic pH determination were used to extract RNA with the Qiagen RNeasy Plant Mini Kit according to the manufacture's instruction. The RNA extractions and all further steps were performed in triplicate. RNA purity was checked by measuring the absorbance ratio (A_{260}/A_{280}). Qiagen's QuantiTec Reverse Transcription Kit was used to reverse-transcribe 10 ng of the isolated RNA according to the manufacturer's instructions. Sigma's SYBR® Green JumpStart™ Taq ReadyMix™ for High Throughput qPCR was used to set up the qPCR reactions. The sample cDNA concentration was 100 ng in a final reaction volume of 20 μL . The final concentration of primers was 2 pmol μL^{-1} for reference genes and genes of interest. Candidate transcripts were amplified with the Rotor Gene 3000 system (Corbett Research, Mortlake, Australia). The Following cycling parameters were chosen: Initial inactivation at 94°C for 2 min; 40 cycles: denaturation at 94°C for 15 s, annealing at primer pairs specific temperature (Appendix Table 1) for 30 s, elongation at 72°C for 30 s. At the end of each cycle the fluorescence signal was measured. After the 40th cycle, a melt-curve analysis (melting: 60-99°C) was performed to control specificity of the primer pairs. All samples and reference genes were run in triplicate. In each run and for each primer pair, a negative template control (NTC) was included to ensure the absence of contamination. In addition, the presence of genomic DNA contamination was excluded by running no RT-controls. The specificity of amplification was confirmed by sequencing.

2.2.9 Gel electrophoresis and immune detection of plasma membrane H⁺-ATPases

The abundance of PM H⁺-ATPases was measured according to Zörb et al. (2005a) with some modifications after separation of isolated vesicle proteins (0.2 µg) by SDS-polyacrylamide gel electrophoresis (SDS-PAGE). After separation of proteins with SDS-PAGE, samples were transferred onto polyvinylidene difluoride (PVDF) membrane filters (0.2 µm, Macherey-Nagel) using a semi-dry blotting system. A polyclonal antibody specific for the central part of plant H⁺-ATPase (Agrisera) was used. Alkaline-phosphatase-conjugated anti-rabbit IgG (Agrisera) was used as secondary antibody. The H⁺-ATPase immunoreactive bands were quantified densitometrically with the software ImageJ 1.49v (National Institutes of Health, USA). Controls and samples were run in triplicate.

2.2.10 Statistical analyses

Data shown are means of four biological replications. Variation among the biological replications is characterized by standard errors (\pm SE). Control and Mg-deficiency treatments were compared using the two-tailed student's t-test. The enzymatic constants were evaluated using a two-way ANOVA, the means were then compared with HSD (SigmaStat 3.5, Systat, Germany).

2.3 Effect of salt stress on plasma membrane H⁺-ATPase activity and its implications for kernel development of maize

2.3.1 Plant cultivation and harvest

Maize plants (*Zea mays* L. cvs. Pioneer 3906 and Fabregas) were cultivated according to Hütsch et al. (2015) using the container technique. 120 L plastic containers were filled with 145 kg of a

Brown Earth subsoil (loamy sand: 15.8% clay, 30.8% silt, 53.4% sand; pH (CaCl₂) 7.1). The topsoil layer was fertilized with a compound fertilizer and micronutrients according to Hütsch et al. (2015). The plants were cultivated in the vegetation hall of the experimental station of the Institute of Plant Nutrition in Giessen under natural light conditions. The containers were set up in a completely randomized design and their position was changed at least once a week. The containers were repeated four times with four plants per container. There were two treatments, a control treatment and a salt stress treatment (NaCl). The salt stress treatment was established by mixing NaCl into the soil to achieve 11 dS m⁻¹ electrical conductivity throughout the soil profile of 90 cm. Silks were hand-pollinated with fresh pollen from unstressed maize plants 5 d after first silk appearance. Just prior to pollination silks were cut 1 cm above the tips of the husk leaves and silk fresh weight was determined. For each individual treatment and genotype three harvests were conducted: Two intermediate harvests were conducted 0 and 2 d after pollination (0 and 2 DAP) and one harvest at kernel maturity. This resulted in different pollination and harvest dates depending on treatment and genotype (Table 1).

Table 1: Harvest of developing kernels: days after sowing (DAS); days after pollination (DAP).

DAS	Treatment
66 DAS	Fabregas Control 0 DAP
68 DAS	Fabregas Control 2 DAP
69 DAS	Fabregas NaCl 0 DAP
71 DAS	Fabregas NaCl 2 DAP
72 DAS	Pioneer 3906 Control 0 DAP
74 DAS	Pioneer 3906 Control 2 DAP
75 DAS	Pioneer 3906 NaCl 0 DAP
77 DAS	Pioneer 3906 NaCl 2 DAP

Plants were harvested according to Hütsch et al. (2015). For each maize genotype and treatment four containers with four plants were harvested (Figure 6). In case a second or third cob developed, it was immediately removed after appearance, the weight recorded and added to the shoot weight.

Shoots were cut into pieces of 10–20 cm and dried at 105°C for 72 h for dry-weight determination. For laboratory analyses, the frozen kernels were ground under liquid N₂ using mortar and pestle and stored at -80°C until further analysis. Due to the difficulty to discriminate between maternal and daughter tissue in the first days after pollination (Wang and Ruan, 2013) in this and other studies enzyme activities and assimilate concentrations were determined in a mixture of maternal tissue (nucellus, pericarp, placenta-chalaza and pedicle) as well as of endosperm and embryonic tissue (Zinselmeier et al., 1999; Hütsch et al., 2014) (Figure 4). In the mature maize plants straw and cob fresh and dry mass, and kernel dry mass (105°C drying), as well as kernel number and kernel weight were determined.



Figure 6: Photograph of a young maize cob 2 d after pollination (DAP).

2.3.2 Sugar determination

An aliquot (100 mg) of frozen, ground kernels was lyophilized for 48 h. Sucrose, glucose, and fructose were analyzed in approximately 10 mg dry weight of pulverized samples. Samples were extracted with 1.8 mL double-deionized water in a shaking heat block at 75°C for 30 min. The

extracts were centrifuged until they were free of plant residues. The supernatants were stored at -20°C. Enzymatic sugar determination was conducted with UV test kits (Boehringer Mannheim/Roche-Biopharm). Each kernel sample was extracted in duplicate prior to sugar analysis. Sugar contents were calculated by multiplication of sugar concentrations and total kernel fresh weights.

2.3.3 Acid invertase enzyme extraction and activity measurements

Extraction of enzymes and incubation for the determination of acid invertase (EC 3.2.1.26) activity were performed according to Zinselmeier et al. (1999) modified by Hütsch et al. (2015). In the present study, only acid invertase activity was determined, since it was shown by Hütsch et al., (2014 and 2015) that activities of other invertases or sucrose synthase (EC 2.4.1.13) were negligible in maize kernels around pollination.

2.3.4 Plasma membrane (PM) isolation of maize kernels

Frozen and ground kernels were used for the isolation of PM vesicles. Otherwise the isolation was conducted in the same manner as described in Chapter 2.2.5 for maize leaves.

2.3.5 Kinetic assays of hydrolytic PM H⁺-ATPase activity of maize kernels

PM H⁺-ATPase hydrolytic activity of maize kernels was determined as described in Chapter 2.2.6 with the exception that the measurements were conducted with 10 mM Mg present in the *in vitro* assay. The activity data were subjected to non-linear regression analysis with DynaFit, as described

in Chapter 2.2.6. However, all data shown here were not normalized and based on a model assuming a Michaelis-Menten relationship which was the best fitting model.

2.3.6 Measurement of proton-pumping activity of PM H⁺-ATPase of maize kernels

Active transport rate, passive transport rate, and maximum pH gradient were measured as described in Chapter 2.2.7.

2.3.7 Relative abundance of RNA plasma membrane H⁺-ATPase isoforms

The qPCR analyses for maize kernel was conducted as described in Chapter 2.2.8 for maize leaf tissue.

2.3.8 Gel electrophoresis and immunodetection of plasma membrane H⁺-ATPase

The abundance of PM H⁺-ATPase was measured according to Zörb et al. (2005a) with modifications (described in Chapter 2.2.9) after separation of isolated vesicle proteins (0.5 µg) with SDS.

2.3.9 Statistical analyses

Means were calculated from four replicates per treatment and genotype. Variation among the biological replications is characterized by standard errors (\pm SE). Planned contrasts were conducted between control and salt stress treatments when *a priori* differences were hypothesized. Significant

differences are indicated by * $P \leq 5\%$, ** $P \leq 1\%$, and *** $P \leq 0.1\%$. Additionally, three-way ANOVAs were conducted to test for unanticipated differences (*a posteriori*). Multiple comparisons separating means in homogenous subgroups were performed using the *post hoc* Tukey test ($P \leq 5\%$). Significant differences are indicated by different small letters. All statistical tests were performed by means of Statistica (version 12, Dell, Inc., USA).

3. Results

3.1 Stumbling blocks for chlorophyll concentration measurements in Mg-deficient plant material

3.1.1 Effect of Mg deficiency on maize growth and N-tester results

At the first harvest (5 DAO), the plant fresh weights were not significantly reduced under low Mg supply. However, for the 3rd leaf that had emerged a decrease of fresh weight under Mg deficiency was observed (control 500 μM Mg = 0.47 ± 0.02 g; Mg deficiency 25 μM Mg = 0.43 ± 0.03 g), becoming significant ($P = 1\%$) 3 d later at the second harvest (8 DAO: control 500 μM Mg = 1.04 ± 0.03 g; Mg deficiency 25 μM Mg = 0.88 ± 0.02 g) (Figure 7). Already at the first harvest (5 DAO), the N-tester-values were reduced significantly for all leaves under low Mg supply (Table 2).

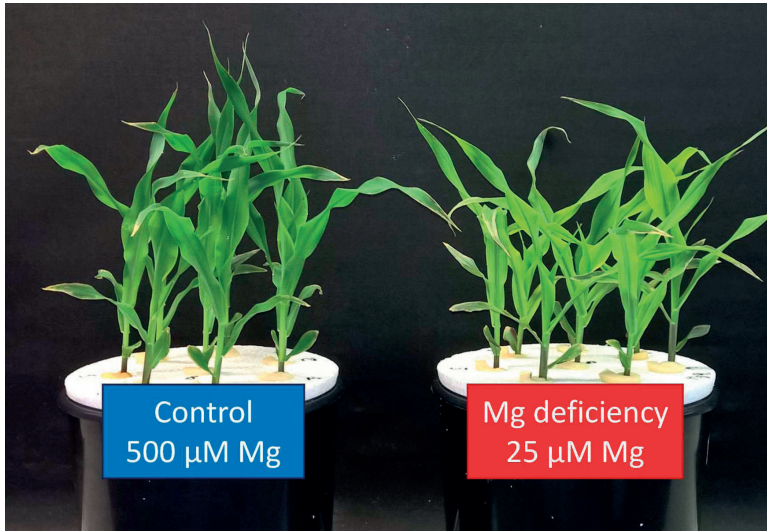


Figure 7 Effect of Mg nutrition on maize appearance 8 d after onset (DAO) of differential Mg treatment; control nutrient solution with 500 μM Mg, Mg deficiency with 25 μM Mg.

Table 2: Effect of Mg nutrition on maize leaf N-tester readings (dimensionless) 5 and 8 d after onset (DAO) of differential Mg treatment; control nutrient solution with 500 μM Mg, Mg deficiency with 25 μM Mg; means ($n = 4$) \pm SE; **P = 1% = ***P = 0.1%; difference in percentage between control and Mg-deficiency treatment on the same harvest date.

Treatment	Harvest	2 nd leaf		3 rd leaf	
Control (500 μM Mg)	5 DAO	552 \pm 10		376 \pm 13	
Mg deficiency (25 μM Mg)		365*** \pm 23	-34%	277** \pm 13	-26%
Control (500 μM Mg)	8 DAO	648 \pm 10		617 \pm 12	
Mg deficiency (25 μM Mg)		320*** \pm 18	-51%	279*** \pm 6	-55%

3.1.2 Effect of addition of MgCO₃ during extraction of maize leaves grown under Mg deficiency on chlorophyll concentrations

The classical destructive method to measure chlorophyll concentration showed always a significant reduction of chlorophyll concentration for the 2nd leaf (Figure 8 A) and the 3rd leaf under Mg deficiency (Figure 8 B). No differences in chlorophyll a and chlorophyll a+b concentrations were observed between samples with and without MgCO₃ addition (Figure 8). However, 8 d after onset of differential Mg treatment (8 DAO), the chlorophyll b concentration of the 3rd leaf decreased slightly but significantly when MgCO₃ had been added before extraction. At the first harvest (5 DAO), only a trend of decrease in chlorophyll b concentration was observed after addition of MgCO₃ (Figure 8). There was no indication that new chlorophyll was formed enzymatically or non-enzymatically from the extracted pigments, when the plant acetone extract was incubated at 25°C for 10 min, or when the plant material was incubated in deionized water at 25°C for 10 min before acetone extraction (data not shown).

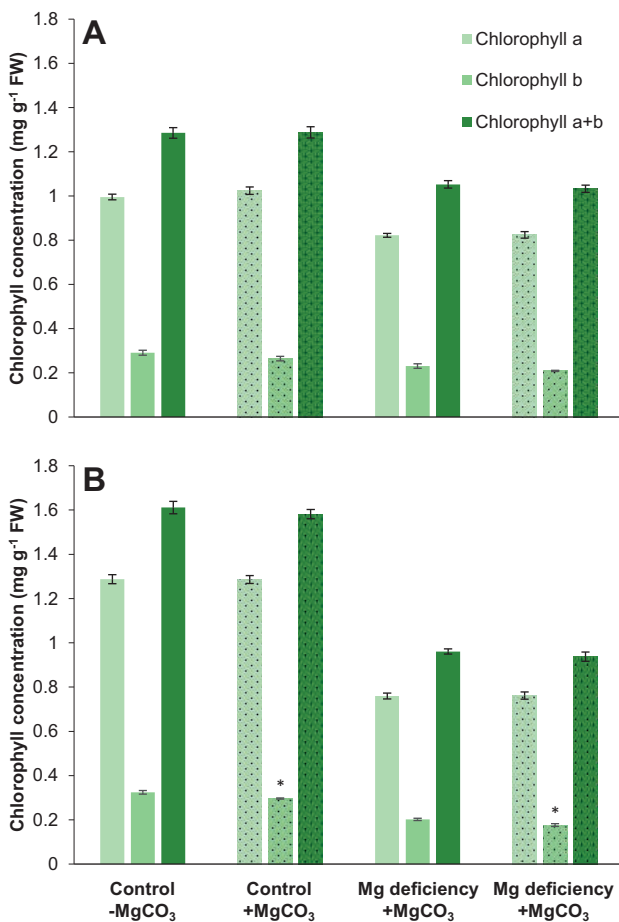


Figure 8: Effect of Mg nutrition on chlorophyll concentrations of the 3rd maize leaf 5 d (A) and 8 d (B) after onset (DAO) of differential Mg treatment; control nutrient solution with 500 μ M Mg, Mg deficiency with 25 μ M Mg, with +MgCO₃ and without -MgCO₃ addition before pigment extraction with aqueous acetone; means (n = 4) \pm SE; differences between treatments extracted with and without MgCO₃ addition during extraction are significant with *P = 5%; significant differences between control and Mg-deficiency treatment not marked in figures with P = 0.1%; FW = fresh weight.

3.2 Effect of Mg deficiency on plasma membrane H⁺-ATPase activity and the implications for maize growth

3.2.1 Effect of slowly developing Mg deficiency on maize growth

The Mg deficiency was induced in the Mg-deficiency treatment right from the start of maize cultivation, when plants were transferred first into nutrient solution. Four days after onset of differential Mg nutrition, the Mg concentration of roots was reduced by 61% relative to control roots; in the 1st and 2nd leaf the Mg concentration was reduced significantly by 30% (Appendix Figure 2). Shoot and root concentrations of potassium and calcium were not significantly affected during the first days (data not shown).

The first evidence of reduced growth was found on days 5-6 after the onset of differential Mg nutrition. The growth rate of the 4th emerged leaf blade was significantly reduced (Figure 9). Leaf blade 4 was not visible yet at onset of Mg deficiency and reached its final size 8 d later. Therefore, leaf 4 was a developing leaf during this timeframe. It is important to note that the final size of each leaf blade was the same at the end. However, leaf growth was delayed in the Mg-deficiency treatment. There was no evidence for a reduction in root fresh weight in the first 10 d after onset of Mg deficiency (Figure 10). Shoot fresh weight production was significantly reduced by Mg deficiency on day 7 (Figure 10). 10 DAO dry weight of leaf blade 3 was significantly higher under Mg deficiency (data not shown). Dry weights of the whole shoot or leaf blade 4 were not altered during the duration of the experiment (data not shown). These results were confirmed by three independent experiments for maize under the described growth conditions.

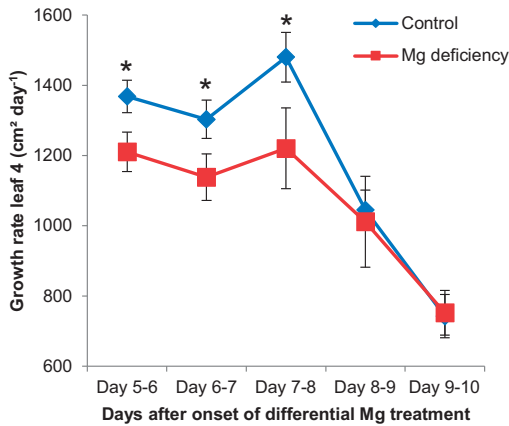


Figure 9: Effect of Mg nutrition on the growth rate of leaf 4 of maize grown with two different Mg treatments. Control (blue) nutrient solution with 500 μM Mg, Mg deficiency (red) with 25 μM Mg. Means ($n = 4$) \pm SE. Significant differences at * $P = 5\%$ between control and the Mg-deficiency treatment.

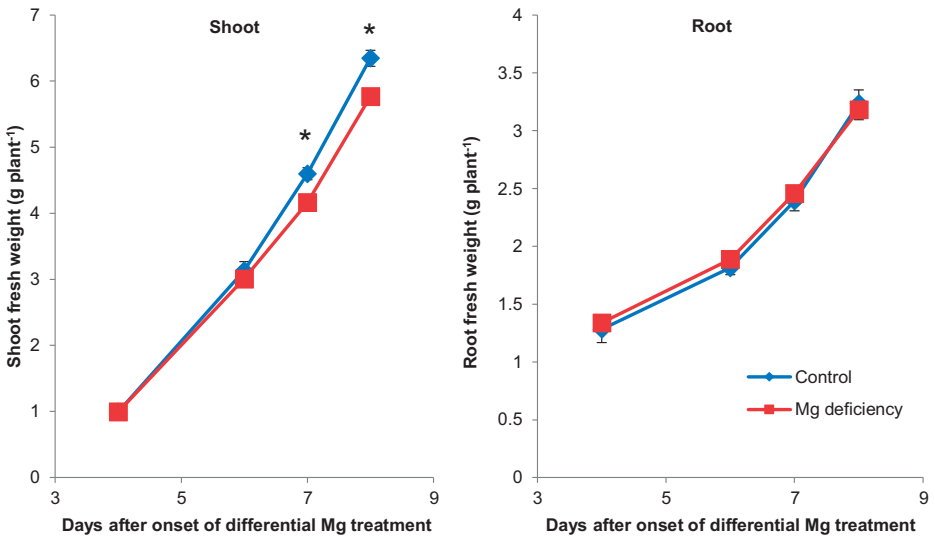


Figure 10: Effect of Mg nutrition on shoot and root fresh weights of maize. Control (blue) nutrient solution with 500 μM Mg, Mg deficiency (red) with 25 μM Mg; means ($n = 4$) \pm SE. Significant differences at * $P = 5\%$ between control and Mg-deficiency treatment.

3.2.2 Effect of Mg deficiency on chlorophyll, sugar, and protein concentrations of maize

The chlorophyll, sugar, and protein concentrations were measured in source and sink tissue, to determine if any of these parameters could have limited growth.

A significant decrease in chlorophyll concentration was found in the older leaves 8 d after onset of differential Mg nutrition (Figure 11). Hence, this difference occurred 3 d after the first measured effect on growth of leaf 4 (Figure 9). A parameter for photosynthesis output is the sugar concentration of leaf blade tissue. The soluble sugars glucose, fructose, and sucrose accumulated in the mature leaves 6 d after onset of treatment (Figure 12). There was no reduction in hexose concentrations in the younger leaves while the leaf blades were still growing (leaf blade 4 and 5) in Mg-deficient plants (Figure 9). There was a clear pattern when leaf blades had reached the final size: First there was an accumulation of sucrose, followed by an accumulation of glucose and fructose. In roots and root tips there was a decrease in sucrose concentration on day 8, but this difference disappeared on day 10 (Figure 12). Therefore, no lasting changes in sugar concentrations were observed during the timeframe when the first decrease in leaf growth occurred.

Protein concentration was measured to assess whether amino acid supply or the translation process itself might be inhibited under Mg deficiency in sink tissues. The concentration of soluble proteins was significantly decreased in the roots of the Mg-deficient treatment on day 8 after the onset of differential Mg nutrition (Figure 13). However, there was no reduction of soluble proteins in root tips. In growing leaves, protein concentrations were not affected by low Mg supply during the timeframe of the experiment, either (Figure 13).

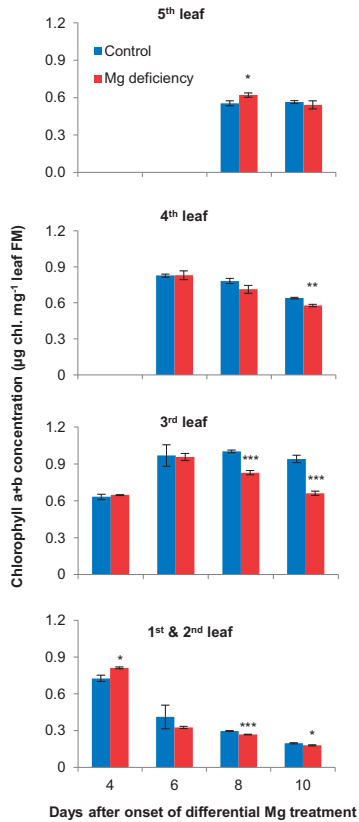


Figure 11: Effect of Mg nutrition on chlorophyll (a + b) concentrations of leaves of maize. Control (blue) nutrient solution with 500 µM Mg and Mg deficiency (red) with 25 µM Mg; means (n =4) ± SE. Significant differences at *P = 5%, **P = 1%, ***P = 0.1% between control and the respective Mg-deficiency treatment.

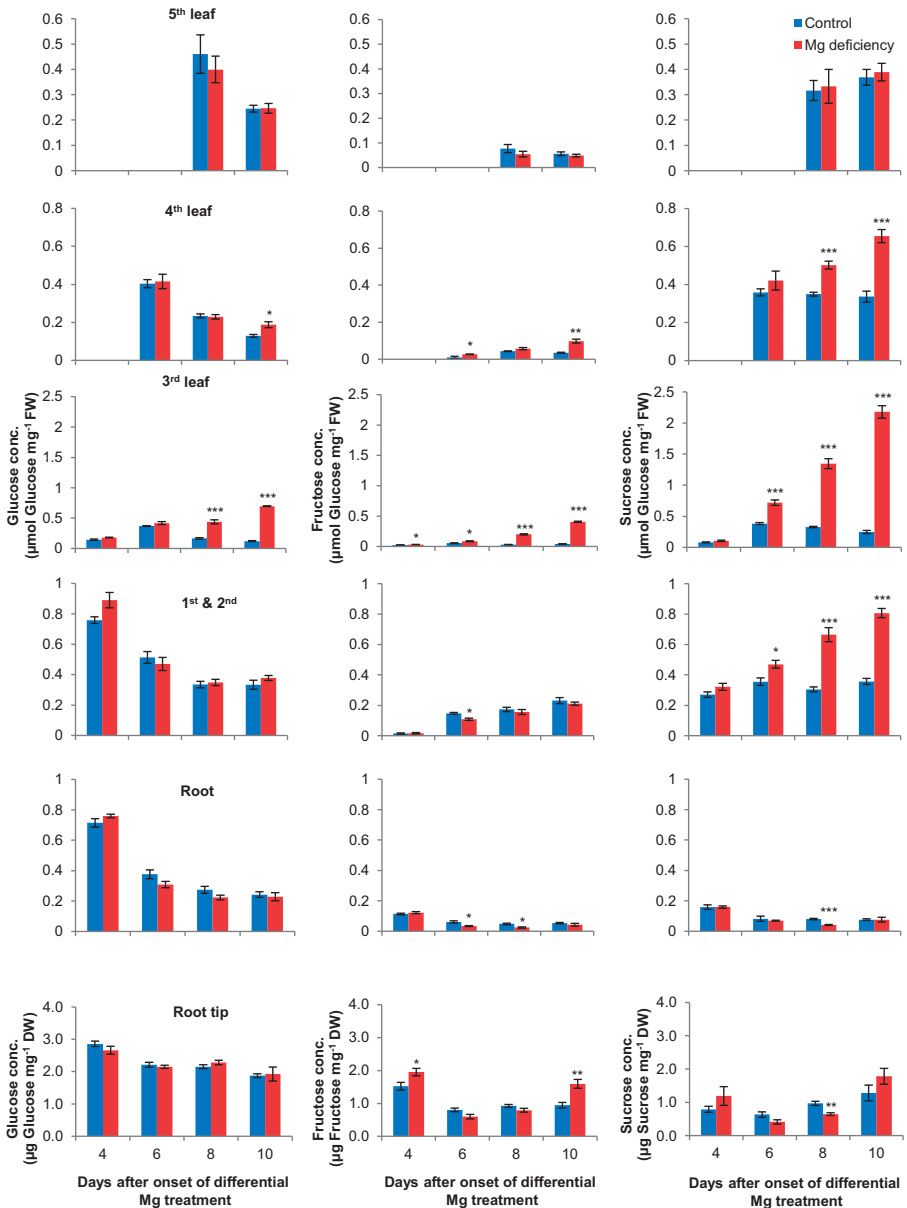


Figure 12: Effect of Mg nutrition on glucose, fructose, and sucrose concentrations of maize. Control (blue) nutrient solution with 500 µM Mg, Mg deficiency (red) with 25 µM Mg; means (n = 4) ± SE. Significant differences at *P = 5%, **P = 1%, ***P=0.1%; FW = fresh weight; DW = dry weight.

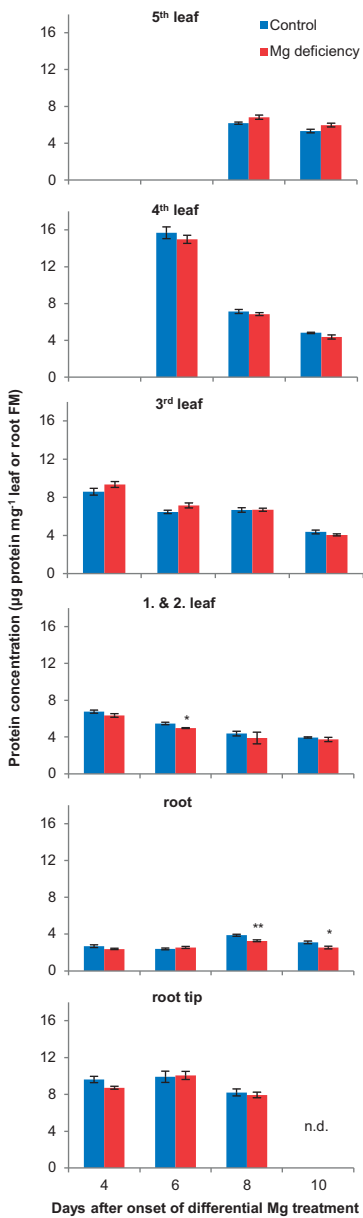


Figure 13: Effect of Mg nutrition on soluble protein concentration of leaves and roots of maize. Control (blue) nutrient solution with 500 µM Mg, Mg deficiency (red) with 25 µM Mg; means (n = 4) ± SE. Significant differences at *P = 5% and **P = 1% between control and the Mg-deficiency treatment.

3.2.3 Effect of Mg deficiency on DNA contents of maize

In order to quantify the effect of Mg deficiency on the process of cell division, DNA contents of leaves and roots were determined. The results show no significant differences in DNA content between control and Mg-deficiency treatments in the growing 5th leaves (Figure 14). There was a slightly reduced DNA content in leaf 4, 8 d after onset of Mg deficiency, however this reduction disappeared on day 10. Hence, when the first reduction in growth of either leaf 4 or 5 occurred, the DNA content was not altered in these leaves.

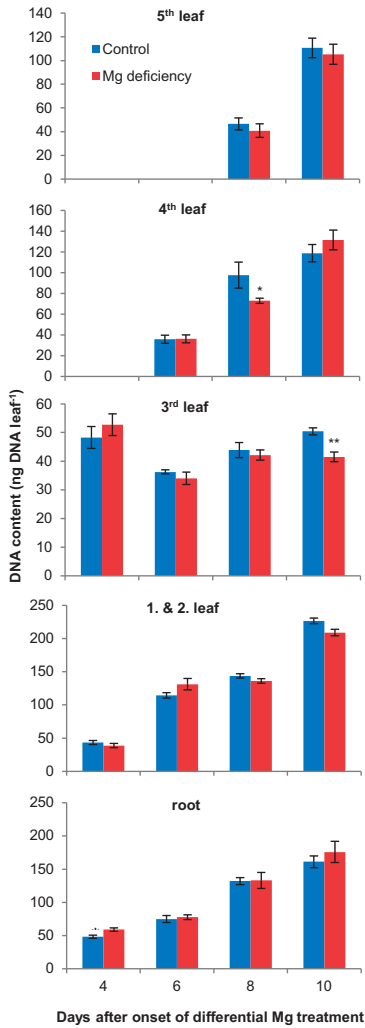


Figure 14: Effect of Mg nutrition on DNA content of leaves and roots of maize. Control (blue) nutrient solution with 500 μM Mg and Mg deficiency (red) with 25 μM Mg; means ($n = 4$) \pm SE. Significant differences at * $P = 5\%$ and ** $P = 1\%$ between control and the Mg-deficiency treatment.

3.2.4 Effect of Mg deficiency on apoplastic pH of young developing leaves

Cell-extension growth was characterized by the parameter growth rate, which was inhibited under Mg deficiency in leaf 4 (Figure 9) 5-6 DAO. One requirement for cell-extension growth is an acidification of the plant's cell wall. Therefore, the apoplastic pH was measured in the growing leaf tissue during the time course of the experiment. The apoplastic pH was significantly higher in growing leaf blades in the Mg-deficient treatment, indicating a lower apoplastic acidification. However, as shown for leaf 4 the difference disappeared when the leaf blade reached its final size. On day 5 and 6, the apoplastic pH was higher for leaf 4, in the Mg-deficient treatment; on day 7 this difference vanished, while for the still growing 5th leaf blade a higher pH was measured (Table 3). Hence, one important prerequisite for cell-extension growth, the acidification of the apoplast was impaired when a reduction in growth was measured in the same tissue.

Table 3: Effect of Mg nutrition on apoplastic pH of maize leaves after onset (DAO) of differential Mg nutrition; means (n = 4) ± SE; significant differences between control (500 μM) and Mg-deficient (25 μM) treatment at each harvest are marked with *P = 5%, **P = 1%, ***P = 0.1%.

	4 DAO (3 rd leaf)	5 DAO (4 th leaf)	6 DAO (4 th leaf)	7 DAO (4 th leaf)	7 DAO (5 th leaf)
Control	5.5 ± 0.0	5.6 ± 0.0	5.6 ± 0.0	6.0 ± 0.0	5.5 ± 0.1
Mg deficiency	5.8* ± 0.0	5.7* ± 0.0	5.8** ± 0.0	6.0 ± 0.0	5.8*** ± 0.1

3.2.5 Effect of Mg deficiency on plasma membrane H⁺-ATPase activity

Plasma membrane (PM) vesicles were isolated from the 4th leaf blades 5 d after onset of treatment. This day and leaf were chosen, because on this day the first sign for leaf growth inhibition in the Mg-deficiency treatment was found and an increase in leaf apoplastic pH was measured which is mainly determined by PM H⁺-ATPase activity (Table 3).

Two different Mg concentrations were used to mimic conditions in the *in vitro* assay: 5 mM to mimic a sufficient Mg supply and 1 mM to mimic a low Mg supply. Plasma membrane H⁺-ATPase of the Mg-deficiency treatment showed a significant higher hydrolytic activity at each given Mg-ATP substrate concentration with 5 mM Mg in the *in vitro* assay compared to vesicles isolated from control plants (Figure 15). This difference in hydrolytic activity between control and Mg-deficiency treatment disappeared with 1 mM Mg used in the *in vitro* assay. The hydrolytic activity decreased when ATP concentrations were higher than the corresponding Mg-assay concentration. The enzymatic constants were calculated after modeling the normalized data from the hydrolytic activity measurements.

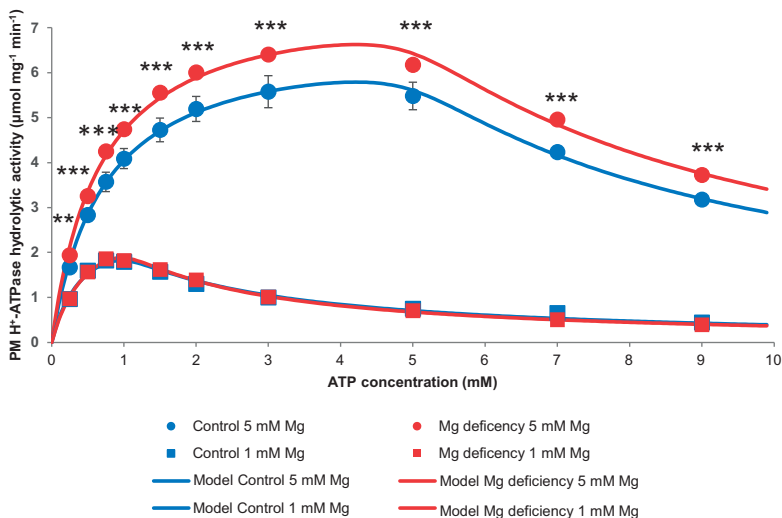


Figure 15: Effect of Mg nutrition on hydrolytic PM H⁺-ATPase activity of leaf 4, 5 d after onset (DAO) of differential Mg nutrition with different ATP and Mg-assay concentrations (1 mM and 5 mM Mg); normalized data; means (n = 4) ± SE; significant differences between control and Mg-deficient treatment at each ATP assay concentration are marked **P = 1% and ***P = 0.1%. Lines show calculated models for each Mg treatment and Mg-assay concentration.

The turnover number (K_r), is the enzymatic constant for the maximum number of chemical conversions of the substrate at a single catalytic site. K_r was higher in the plant material derived from the Mg-deficiency treatment compared to the control with 5 mM Mg in the *in vitro* assay (Table 4). K_r was significantly lower with 1 mM Mg in the *in vitro* assay and the difference between control and Mg-deficiency treatment vanished. The calculated affinity of the H⁺-ATPase to its substrate Mg-ATP (K_m) did not significantly differ between control and Mg deficiency at 5 or 1 mM Mg in the assay, respectively. However, the K_m in the control treatment was lower under 1 mM Mg assay concentration than with 5 mM Mg assay concentration. Although in the Mg-

deficiency treatment the K_m was lower at 1 mM Mg assay concentration compared to 5 mM Mg, this difference was not significant under the tested *in vitro* conditions.

Table 4: Effect of Mg nutrition on PM H⁺-ATPase enzymatic parameters of isolated PM vesicles from leaf 4: catalytic rate constant K_r and Michaelis constant K_m 5 d after onset (DAO) of differential Mg treatment (25 μ M or 500 μ M Mg) were calculated for two Mg assay concentrations from normalized data, assuming competitive substrate inhibition; means (n = 4) \pm SE; small letters indicate significant differences between the treatments and Mg assay concentrations at P = 5% by HSD-test.

	5 mM Mg	1 mM Mg
K_r Control (s⁻¹)	66 \pm 5 b	31 \pm 1 c
K_r Mg deficiency (s⁻¹)	80 \pm 2 a	35 \pm 3 c
K_m Control (μM ATP)	712 \pm 27 a	474 \pm 35 b
K_m Mg deficiency (μM ATP)	682 \pm 23 a	587 \pm 110 a

In order to characterize the PM H⁺-ATPases proton pumping activity, the parameters active H⁺ transport rate, passive H⁺ transport rate and maximum pH gradient were measured. No significant differences in the active H⁺ transport rate or in the passive H⁺ transport rate were detectable (Table 5). However, a higher maximum pH gradient between the inside and the outside of the isolated vesicles was measured with 5 mM Mg present in the *in vitro* assay in the Mg-deficiency treatment. The higher hydrolytic activity and the higher maximum pH gradient in the Mg-deficiency treatment indicate an adaption of the PM H⁺-ATPase under Mg deficiency. The PM H⁺-ATPase activity is altered in the same tissue and on the same day after onset of Mg deficiency on which apoplastic acidification and leaf extension-growth was impaired.

Table 5: Effect of Mg nutrition on PM H⁺-ATPase active H⁺ transport, max. pH gradient and passive H⁺ transport in isolated PM vesicles from leaf 4, 5 d after onset (DAO) of differential Mg treatment (25 μM or 500 μM Mg) at Mg-assay concentration of 5 mM; means (n = 3) ± SE; significant differences between control and Mg-deficiency treatment are marked with *P = 5%.

	Active H ⁺ transport rate (influx) (ΔA_{492} μg protein ⁻¹ min ⁻¹)	Max. H ⁺ gradient (ΔA_{492})	Passive H ⁺ transport rate (efflux) (ΔA_{492} μg protein ⁻¹ min ⁻¹)
Control	0.10 ± 0.03	0.046 ± 0.004	0.28 ± 0.05
Mg deficiency	0.20 ± 0.03	0.057* ± 0.003	0.41 ± 0.04

In order to investigate why the PM H⁺-ATPase activity was altered in the Mg-deficiency treatment compared to the control, the total abundance of the protein was measured. However, the western-blot analyses of H⁺-ATPase protein in plasma-membrane vesicles revealed no change in the total abundance of the protein (Figure 16). Therefore, it was examined whether the relative RNA abundance of different PM H⁺-ATPase isoforms was altered. Transcription of five of six isoforms was confirmed in the investigated segment of leaf 4 (Figure 17). A higher relative abundance of *MHA4* was found 4 d after onset of differential Mg nutrition in the Mg-deficiency treatment compared to the control. The higher relative abundance of *MHA4* was also found 5 d after onset of differential Mg nutrition but disappeared on day 6 after onset of differential Mg nutrition. All investigated isoforms showed a lower abundance (except *MHA5*) under Mg deficiency compared to the control on day 6.

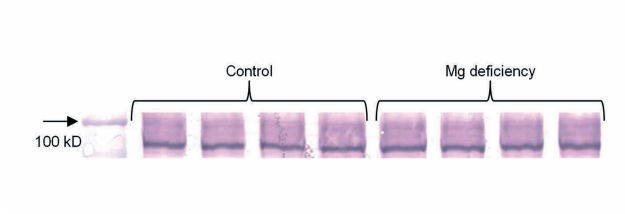


Figure 16: Effect of Mg nutrition on PM H⁺-ATPase protein abundance in isolated PM vesicles of leaf 4, 5 d after onset (DAO) of differential Mg treatment (500 μM = control and 25 μM Mg = Mg deficiency); no significant differences were found.

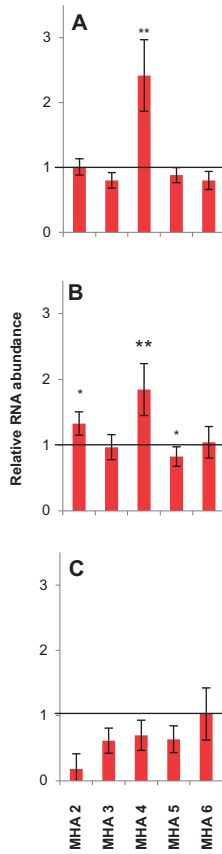


Figure 17: Effect of Mg nutrition on relative RNA abundance of PM H⁺-ATPase isoforms of leaf 4, 4 d (A), 5 d (B), 6 d (C) after onset (DAO) of differential Mg treatment; means (n = 4) ± SE; significant differences between control and Mg-deficiency treatment at each harvest are marked with *P = 5%, **P = 1%.

The time course of the physiological responses of young maize plants subjected to Mg deficiency is summarized in Figure 18.

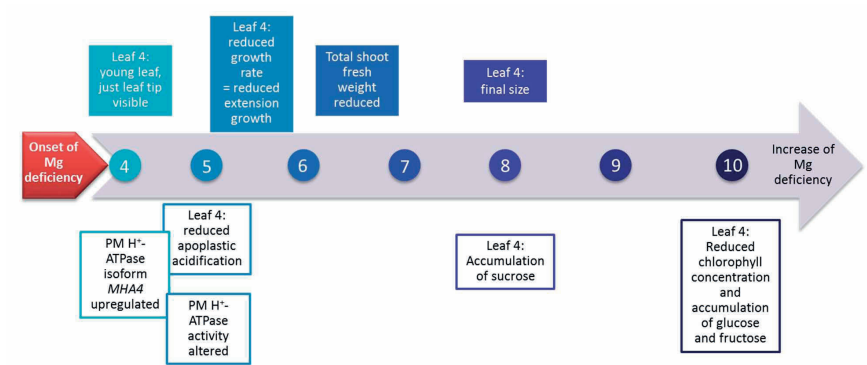


Figure 18: Summarized effects of Mg deficiency on maize. Numbers indicate days after onset (DAO) of Mg deficiency.

3.3 Effect of salt stress on plasma membrane H⁺-ATPase activity and its implications for kernel development of maize

3.3.1 Effect of salt stress on maize yield determinants

Maize was cultivated under control conditions and salt stress in order to determine the reasons for grain-yield reduction at plant maturity. Therefore, maize kernel development and grain yield formation were investigated 0 and 2 d after pollination (DAP) as well as at plant maturity.

As expected, the grain yield of both genotypes was reduced in the salt-stress treatment compared to the control (Figure 19 A). However, the reasons for the yield reduction were different for the genotypes. There was a lower kernel number at the apical part of the cobs in the salt stress treatment (Figure 19 B and Figure 20), with a stronger reduction of kernels for Pioneer 3906 than for Fabregas (Figure 19 B). The kernel fresh weight showed a different picture, with no change for Pioneer 3906 and a reduction for Fabregas in the salt-stress treatment. This reduction in kernel weight for Fabregas was already discussed in an earlier study (Hütsch et al., 2015). In conclusion, the two yield determinants kernel number and kernel weight were affected differently by salt stress for the two genotypes. In order to investigate why the kernel number was reduced at maturity, the physiological reasons for kernel abortion were investigated 0 and 2 DAP.

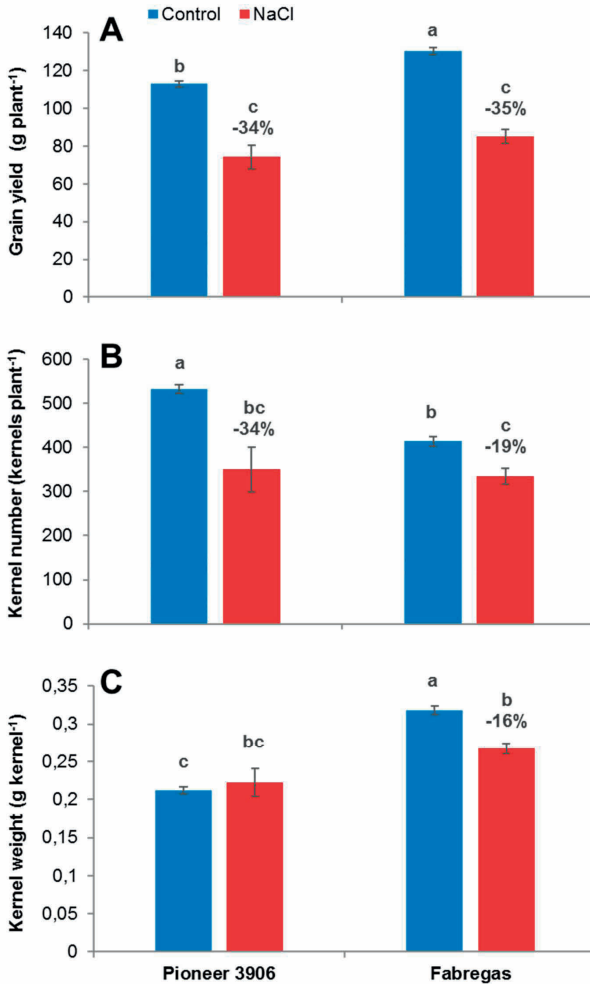


Figure 19: Effect of salt stress on grain yield (A), kernel number (B), and kernel weight (C) at kernel maturity of two maize cultivars (Pioneer 3906 and Fabregas); data show means of four replicates \pm S.E.; difference in percentage between control and stress treatment of one cultivar is given, and significant differences are indicated by different letters regarding all experimental factors (ANOVA and *post-hoc* HSD test).

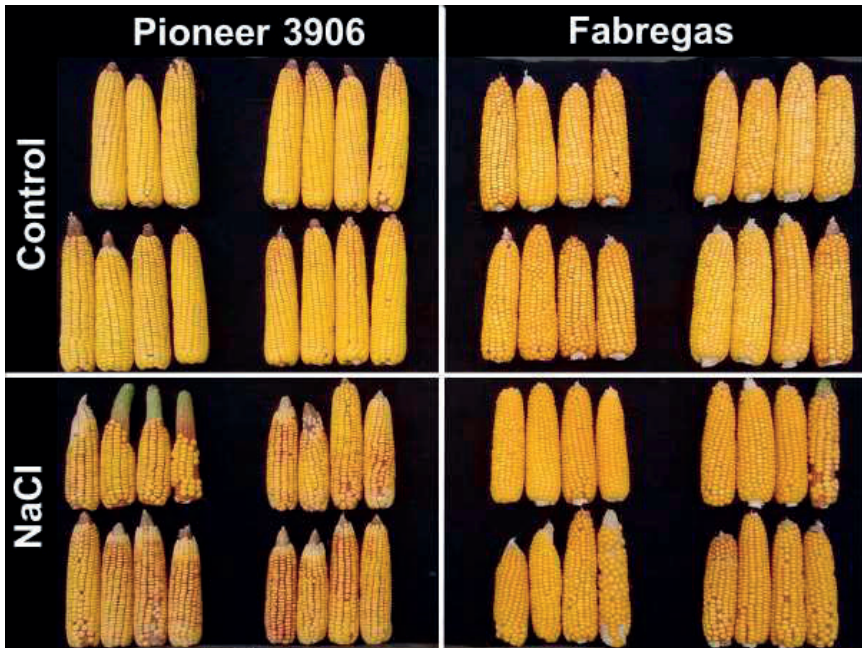


Figure 20: Maize cobs of two cultivars (Pioneer 3906 and Fabregas) at maturity after growth under control conditions and salt stress (EC: 11 dS m⁻¹).

The vegetative shoot growth (straw fresh weight) of both genotypes was significantly reduced due to salt stress compared to the control (Figure 21 C). However, at pollination (0 DAP) no difference in cob or kernel fresh weight was measurable, regardless of the genotype (Figure 21 A, B). Just two days later (2 DAP) the cob and kernel fresh weights were significantly reduced for both genotypes under salt stress (Figure 21 A, B).

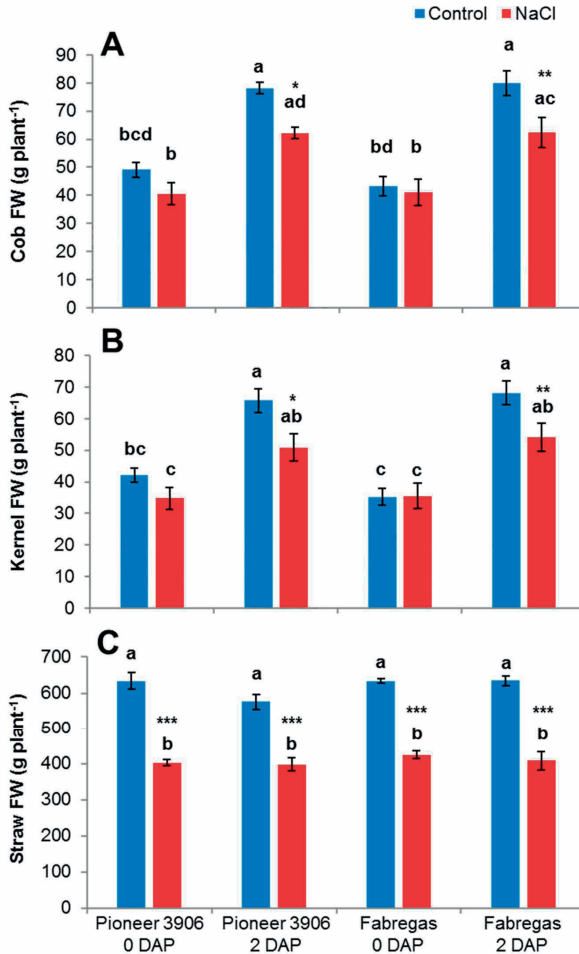


Figure 21: Effect of salt stress on maize fresh weight (FW) (A) kernel FW (B), and straw FW (C) of two corn cultivars (Pioneer 3906 and Fabregas) 0 and 2 d after pollination (DAP); data show means of four replicates \pm S.E.; significant differences between control and salt stress treatment of one cultivar at the same harvest date are indicated by *P = 5 %, **P = 1 % and ***P = 0.1% (*a priori* planned contrasts), and by different letters regarding all experimental factors (ANOVA and *post-hoc* HSD test).

Silk fresh weight was determined at the day of pollination for each individual treatment and genotype. Silk fresh weight was reduced for both genotypes (Figure 22). However, the reduction was much stronger for Pioneer 3906 than for Fabregas under salt stress.

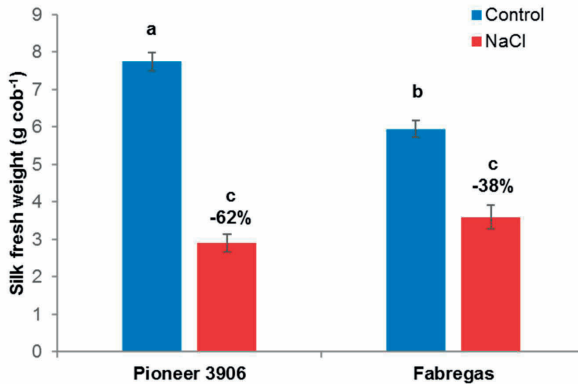


Figure 22: Effect of salt stress on silk fresh weight of two maize cultivars (Pioneer 3906 and Fabregas) 0 d after pollination (DAP); data show means ($n=4$) \pm SE; different letters indicate significant differences regarding all experimental factors (ANOVA and *post-hoc* HSD test).

3.3.2 Effect of salt stress on maize kernel sugar metabolism

The concentrations of soluble sugars in the tissue of developing kernels were determined because sugar availability is one of the main determinants for successful kernel development in the first days after pollination. The hexose concentrations (glucose and fructose) were higher under salt stress regardless of harvest date or genotype (Figure 23 A, B). The sucrose concentrations were also higher under salt stress, with larger differences to the control at 0 DAP than at 2 DAP (Figure

23 C). The hexose contents did not differ significantly, when comparing the salt stress treatments with their corresponding controls (Figure 24 A, B). However, 2 DAP the glucose and fructose contents were often significantly higher compared to 0 DAP (Figure 24 A, B). The sucrose contents were significantly higher under salt stress at 0 DAP for both genotypes, whereas no difference was found between control and salt stress at 2 DAP (Figure 24 C).

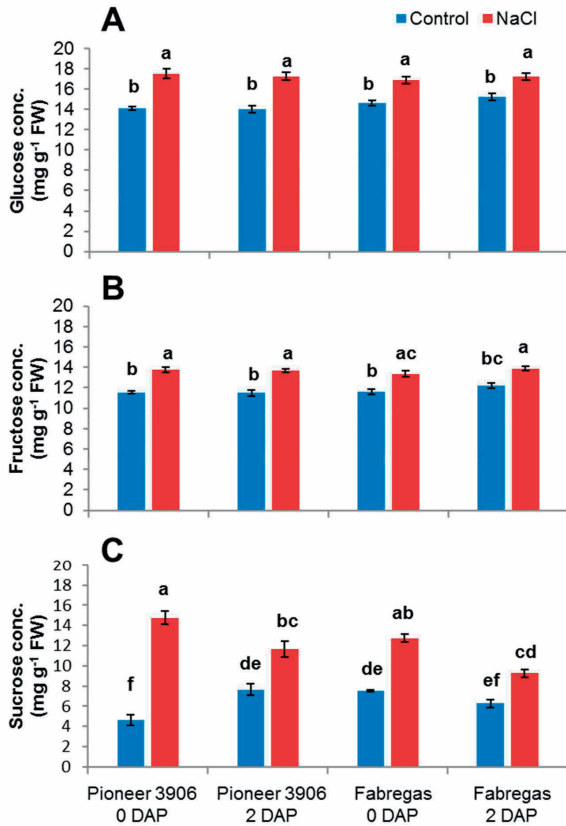


Figure 23: Effect of salt stress on glucose (A), fructose (B), and sucrose (C) concentrations of kernels of two maize cultivars (Pioneer 3906 and Fabregas) 0 and 2 d after pollination (DAP); data show means (n=4) \pm SE; different letters indicate significant differences regarding all experimental factors (ANOVA and *post-hoc* HSD test).

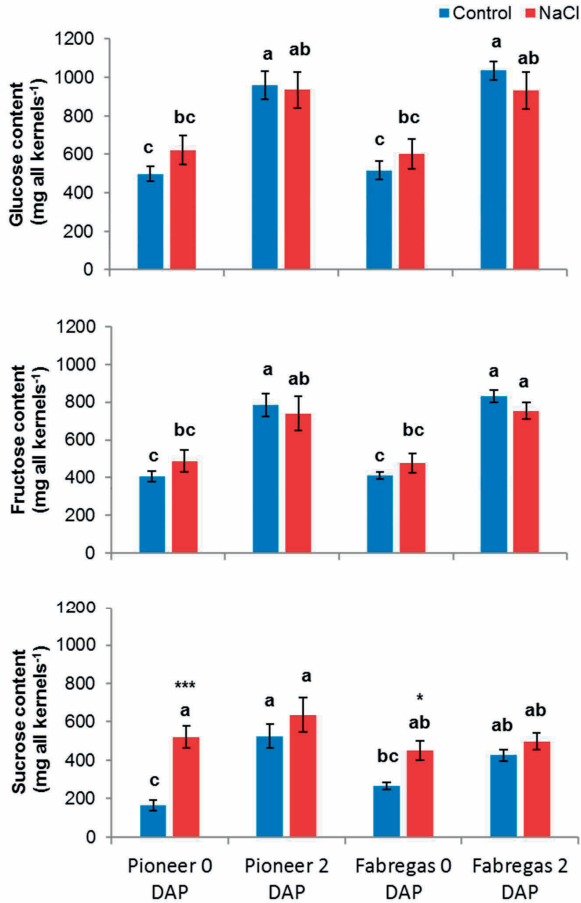


Figure 24: Effect of salt stress on glucose (A), fructose (B), and sucrose (C) contents of kernels of two maize cultivars (Pioneer 3906 and Fabregas) differences between control and salt stress treatment of each individual genotype and harvest are indicated by * $P = 5\%$ (*a priori* planned contrasts), and by different letters regarding all experimental factors (ANOVA and *post-hoc* HSD test).

In line with the high sucrose concentrations at 0 DAP under salt stress (Figure 23 C), the *in vitro* acid invertase activity was strongly reduced by 68% for Pioneer 3906 and 46% for Fabregas (Figure 25). However, 2 DAP there was no difference in the *in vitro* acid invertase activity between control and salt stress of either genotype (Figure 25), although the sucrose concentrations were also higher in the salt-stress treatment (Figure 23 C). Additionally, the activity in the controls of both genotypes was significantly higher at 0 DAP compared to 2 DAP (Figure 25).

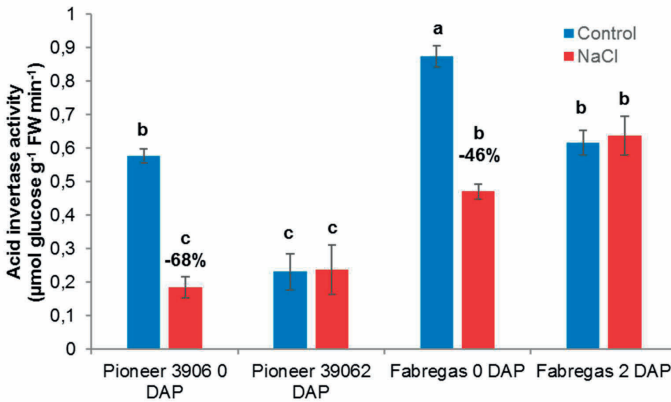


Figure 25: Effect of salt stress on *in vitro* acid invertase activity of kernels of two maize cultivars (Pioneer 3906 and Fabregas) 0 and 2 d after pollination (DAP); data show means (n=4) ± SE; difference in percentage between control and stress treatment of one cultivar at the same harvest date is given, and significant differences are indicated by different letters regarding all experimental factors (ANOVA and *post-hoc* HSD test).

3.3.3 Effect of salt stress on maize kernel PM H⁺-ATPase activity

Since the PM H⁺-ATPase is important for the uptake of hexoses into the kernel cytoplasm, kernel PM vesicles were isolated to characterize the PM H⁺-ATPase activity *in vitro*.

The hydrolytic activity of the PM H⁺-ATPase was characterized by a kinetic model of the enzyme which allowed to calculate the kinetic parameters K_r and K_m. K_r describes the maximum turnover

rate of the substrate Mg-ATP at the enzyme binding site and K_m characterizes the affinity of the enzyme to its substrate. The calculations of these constants were performed by fitting a model to the measured activity data assuming a Michaelis-Menten relationship. At time of pollination (0 DAP) Pioneer 3906 showed no significant difference in the hydrolytic activity between salt stress and control treatment (Table 6 and Figure 26 A). However, 2 DAP the hydrolytic activity was higher compared to 0 DAP, regardless of the treatment. In addition, 2 DAP the hydrolytic activity was significantly lower in the salt stress treatment compared to the corresponding control (Table 6 and Figure 26 A). A significantly reduced activity under salt stress compared to the control treatment was also observed for Fabregas 2 DAP (Table 6 and Figure 26 B). In contrast to Pioneer 3906, 0 DAP a higher hydrolytic activity was observed for the stress treatment of Fabregas kernels compared to the control (Figure 26 B). No significant difference was observed for the affinity of the isolated PM H^+ -ATPase enzyme to its substrate: The level of the K_m constant was similar for each treatment, harvest date and genotype (Table 6).

Table 6: Effect of salt stress (EC: 11 dS m⁻¹) on PM H^+ -ATPase kinetic parameters of isolated PM vesicles from kernels of two maize cultivars (Pioneer 3906 and Fabregas): catalytic rate constant K_r and Michaelis constant K_m ; means ($n = 3-4 \pm SE$; significant differences between control and salt-stress treatment of one cultivar at the same harvest date are indicated by * $P = 5\%$ (*a priori* planned contrasts), and by different letters regarding all experimental factors (ANOVA and *post-hoc* HSD test).

	Pioneer 3906 0 DAP	Pioneer 3906 2 DAP	Fabregas 0 DAP	Fabregas 2 DAP
K_r Control (s⁻¹)	48 ± 6 b	74 ± 2 a	44 ± 2 b	58 ± 4 ab
K_r NaCl (s⁻¹)	52 ± 6 b	61* ± 1 ab	56* ± 4 ab	44* ± 2 b
K_m Control (μM ATP)	1255 ± 159 a	994 ± 108 a	1130 ± 76 a	1157 ± 314 a
K_m NaCl (μM ATP)	1343 ± 314 a	1019 ± 63 a	955 ± 66 a	848 ± 59 a

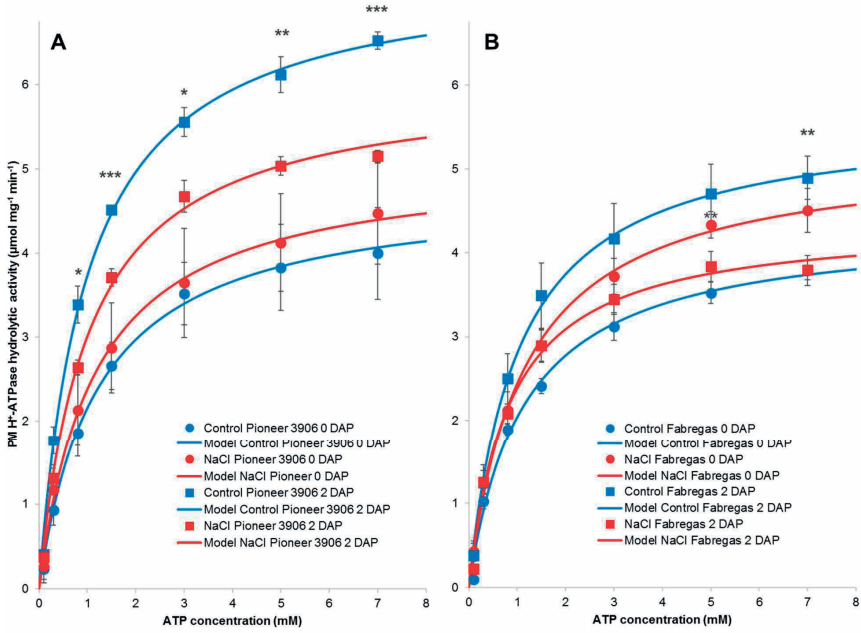


Figure 26: Effect of salt stress on PM H⁺-ATPase hydrolytic activity in isolated plasma-membrane vesicles of developing kernels of maize cultivars Pioneer 3906 (A), and Fabregas (B) 0 and 2 d after pollination (DAP); data show means (n=4) ± S.E.; Significant differences between control and salt stress treatment of each individual harvest are indicate by *P = 5 %, **P = 1 and ***P = 0.1% (*a priori* planned contrasts).

The pH gradient of isolated PM vesicles is established by the PM H⁺-ATPase, which is measured as the quenching of absorbance by acridine orange (AO) at 492 nm (ΔA_{492}), after addition of Mg-ATP as substrate. The active H⁺ transport rate (influx) was significantly higher 2 DAP compared to 0 DAP, regardless of genotype or treatment (Table 7). No difference was found between the salt-stress treatment and its corresponding control (Table 7). The maximum pH gradient was also higher

2 DAP for Pioneer 3906 compared to each respective treatment at 0 DAP. For Pioneer 3906 the max. pH gradient was significantly lower in the salt stress treatment compared to the respective control 2 DAP (Table 7). No other significant differences in the max. pH gradient between controls and their corresponding salt stress treatments were observed (Table 7). The passive H⁺ transport rate (efflux), a measure for the leakage of protons out of the isolated PM vesicles, was not altered by treatment, genotype, or harvest date (Table 7).

Table 7: Effect of salt stress (EC: 11 dS m⁻¹) on PM H⁺-ATPase active H⁺ transport, max. pH gradient and passive H⁺ transport in isolated PM vesicles from kernels of two maize cultivars (Pioneer 3906 and Fabregas); means (n = 3-4) ± SE; significant differences between control and salt-stress treatment of one cultivar at the same harvest date are indicated by *P = 5% (*a priori* planned contrasts), and by different letters regarding all experimental factors (ANOVA and *post-hoc* HSD test).

		Pioneer 3906 0 DAP	Pioneer 3906 2 DAP	Fabregas 0 DAP	Fabregas 2 DAP
Active H⁺ transport rate (influx) (ΔA_{492} $\mu\text{g protein}^{-1}$ min^{-1})	Control	0.21 ± 0.03 d	0.85 ± 0.06 a	0.12 ± 0.02 d	0.58 ± 0.02 c
	NaCl	0.23 ± 0.06 d	0.76 ± 0.02 ab	0.14 ± 0.02 d	0.62 ± 0.04 bc
Max. pH gradient (ΔA_{492})	Control	0.048 ± 0.005 bcd	0.065 ± 0.002 a	0.040 ± 0.002 cd	0.051 ± 0.001 bc
	NaCl	0.046 ± 0.001 bcd	0.058* ± 0.001 ab	0.037 ± 0.002 d	0.048 ± 0.001 bcd
Passive H⁺ transport rate (efflux) (ΔA_{492} $\mu\text{g protein}^{-1}$ min^{-1})	Control	0.28 ± 0.05 a	0.45 ± 0.04 a	0.34 ± 0.03 a	0.35 ± 0.04 a
	NaCl	0.35 ± 0.03 a	0.36 ± 0.03 a	0.30 ± 0.05 a	0.26 ± 0.04 a

The relative RNA abundance of PM H⁺-ATPase isoforms was assessed as a measure of PM H⁺-ATPase adaption under salt stress at the transcriptional level. The PM H⁺-ATPase isoforms *MHA2* – *MHA5* were measurably expressed in the kernel tissue at the transcriptional level. However, with the exception of Fabregas 2 DAP (*MHA 4* and *MHA5*) no significant differences in the relative expression were observed between control and salt stress treatment (Figure 27).

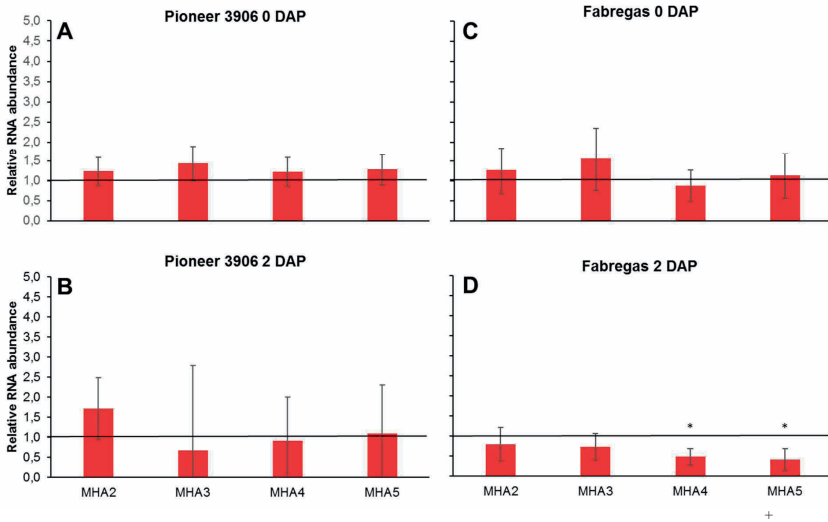


Figure 27: Effect of salt stress on relative RNA abundance of four different PM H⁺-ATPase isoforms isolated from developing maize kernels. Pioneer 3906 0 DAP (A), Pioneer 3906 2 DAP (B), Fabregas 0 DAP (C), and Fabregas 2 DAP (D) (DAP = days after pollination); data show means (n=4) ± SE; significant differences between control and salt stress are indicated by *P = 5%.

The total abundance of H⁺-ATPase protein of the isolated PM vesicles was assessed by western-blot analyses with specific H⁺-ATPase antibodies. Whereas no significant difference in band intensity was found for Fabregas, for Pioneer 3906 a reduction by 12% was found in the salt-stress treatment compared to the control 2 DAP (Figure 28).

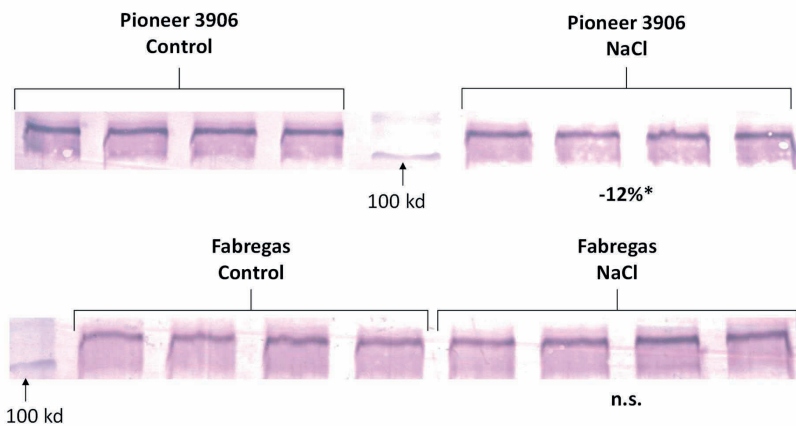


Figure 28: Effect of salt stress ($EC: 11 \text{ dS m}^{-1}$) on total protein abundance of PM H^+ -ATPase of vesicles isolated from maize kernels of Pioneer 3906 2 d after pollination (DAP); data show means ($n = 4$) \pm SE; difference in percentage between control and salt-stress treatment is given; Control and salt stress treatment were compared using two-sample student's t-test (* $P = 5 \%$).

4. Discussion

The aim of this study was to characterize the physiological response of PM H⁺-ATPase to abiotic stress in vegetative and generative plant tissue. More precisely the effect of Mg deficiency on maize vegetative growth as well as the effect of salt stress on maize grain yield development were examined with a focus on the alterations of PM H⁺-ATPase activity and the impact of these alterations on plant physiology.

4.1 The photometric standard method using acetone extracts to determine chlorophyll is applicable to Mg-deficient maize tissue

One goal of this study was to evaluate a standard method for chlorophyll measurements, since the correct determination is essential to characterize the chronology of the impact of Mg deficiency on plant physiological processes. The concern with the standard method was that due to the addition of MgCO₃ as a pH buffer during acetone extraction of pigments, Mg might be inserted into pheopigments of Mg-deficient leaf tissue, resulting in an overestimation of the chlorophyll concentration in this tissue. However, the results clearly showed that the chlorophyll a+b concentrations were identical, whether MgCO₃ was added before extraction or not (Figure 8). This was the case under normal extraction conditions and also when the leaf material was incubated (at 25°C for 10 min) prior to pigment extraction (data not shown). In a pretest (data not shown), it was assessed if Mg from MgCl₂ or MgCO₃ could be inserted into pure pyropheophorbide dissolved in an aqueous acetone solution under different conditions (temperature, concentration, and incubation time). From this pretest it was concluded that it is not possible to insert Mg from MgCO₃ under these conditions without catalyzing the reaction enzymatically. However, it was previously described that this is possible - non-enzymatically - using highly reactive methylmagnesium iodide

as a Mg donor, to insert Mg into pheophytin successfully (Willstätter and Stoll, 1913) resulting in new-formed chlorophyll.

During the extraction process, enzymatic activity is still possible (e.g., chlorophyllase activity; Hu et al., 2013). Therefore, it could not be ruled out beforehand that the Mg chelatase catalyzed the insertion of Mg into protoporphyrin IX during the extraction process in aqueous acetone. In this study, Mg-chelatase activity was not measured directly, so it is also possible that Mg chelatase was still functional, but the lack of substrates, either ATP or protoporphyrin IX, prohibited a possible catalytic function. Likewise, pheophorbide inhibits Mg chelatase during senescence (Pöpperl et al., 1997). Since pheophytin and chlorophyll can lose the phytol chain during extraction with organic solvents (due to chlorophyllase activity) and are thus converted to pheophorbide and chlorophyllide (Hu et al., 2013), this inhibition of Mg chelatase could actually occur in the acetone extract. Precursors of chlorophylls and degradation products are strong photo-sensitizers and therefore their concentration is tightly controlled. During chlorophyll degradation in the course of leaf senescence or fruit ripening, pheophytin and pheophorbide are rapidly metabolized to avoid oxidative stress (Kräutler, 2008; Hörtensteiner and Kräutler, 2011). Consequently, it is unlikely that there was a high concentration of protoporphyrin IX in Mg-deficient leaves. It can be concluded that there were no differences in photometrically determined chlorophyll a and chlorophyll a+b concentrations, whether MgCO₃ was added or not (Figure 8). Therefore, Mg-chelatase activity during the extraction process was unlikely and no new chlorophyll was formed during the extraction process. Consequently, the method is suitable for the determination of chlorophyll concentrations in Mg-deficient leaves. Due to the fact that chlorophyll a+b concentrations were the same, whether MgCO₃ was added or not (Figure 8), there is no need to add MgCO₃ for extract-buffering. Some

authors recommended to use pH-buffered acetone [80% (v/v) acetone with 20% (v/v) 0.2 M Tris-HCl, pH 8]. The alkaline pH may exclude the possibility of displacement of Mg from chlorophyll molecules by protons (Hu et al., 2013).

The chlorophyll meter (N-tester) measurements showed a higher decrease (in %) in chlorophyll concentration, compared to the destructive photometric measurements, when control and Mg-deficient leaves were compared (Table 2). However, plenty of studies (e.g., Bullock and Anderson, 1998; Koning et al., 2015) showed that there is a high correlation between N-tester values and the chlorophyll concentrations measured photometrically after pigment extraction with organic solvents. The N-tester measurements showed that the values are also reliable for plants grown under Mg deficiency. It can also be ruled out that the synthesis of anthocyanins in Mg-deficient leaves overlapped the chlorophyll breakdown and biased the N-tester results.

In conclusion, both methods, non-destructive N-tester readings and photometric chlorophyll determination after aqueous acetone extraction proved to be reliable methods for the determination of chlorophyll in Mg-deficient leaves. For chlorophyll extraction, MgCO₃ addition is not required but it is recommended to buffer the pH of the extraction medium in an alkaline range to avoid exchange of Mg ions from the chlorophyll against protons. The hypothesis that “the photometric standard method using acetone extracts to determine chlorophyll is applicable to Mg-deficient maize tissue,” was accepted.

4.2 Reduced assimilate availability in growing sink tissue is responsible for early growth inhibition under Mg deficiency in maize

One objective of this study was to identify the most sensitive process that is impaired in maize under Mg deficiency and that primarily limits the vegetative growth of maize during insufficient Mg supply. One of these sensitive physiological processes might be the plants sugar metabolism.

The accumulation of sugars in leaf tissue has been described as an early sign of Mg deficiency (Cakmak et al., 1994a; Cakmak et al., 1994b; Hermans et al., 2004a; Hermans et al., 2004b; Hermans and Verbruggen, 2005; Mengutay et al., 2013). Since sugars from photosynthetically active source leaves are an important energy source for the development of sink leaves and the only energy source for roots, they are essential for both growth processes: Cell division and cell-extension growth (Wang and Ruan, 2013). Cakmak et al. (1994a, 1994b) ascribed the accumulation of sugars in leaves to an inhibition of phloem loading, which requires the establishment of a pH gradient by H⁺-ATPase activity. Under Mg deficiency, the substrate Mg-ATP may limit H⁺-ATPase activity and thus phloem loading. The authors mentioned above found a change in sugar partitioning after 11 d of differential Mg treatment in *Arabidopsis* (Hermans and Verbruggen 2005), for beans after 6 d (Cakmak and Kirkby, 2008), and for sugar beet after 12 d (Hermans et al. 2004) of Mg deficiency. An accumulation of sugars in the older maize leaves was found in this study, too. However, there was no consequent decrease in sugar concentrations in the younger growing leaves (Figure 12), when the first growth inhibition occurred (Figure 9). Therefore, sugars are not the limiting factor for the early leaf-growth reduction in the Mg-deficiency treatment.

A reduction of the protein concentration would indicate a possible shortage of amino acids or an inhibition of the translation process itself. It has been shown that Mg assists during assembly of

ribosome subunits in the translation process (Kiss, 1988). Jezek et al. (2015) also found that protein concentrations of maize were not affected by severe Mg deficiency over 54 d. They concluded that, even though the free amino acid concentrations were higher under Mg deficiency, protein synthesis was not the limiting factor for growth. In this experiment, the translation process was not limited by Mg deficiency either (Figure 13). This clearly shows that neither assimilate production nor assimilate availability in sink tissues was primarily limiting growth under Mg deficiency. Therefore, the hypothesis that “reduced assimilate availability in growing sink tissue is responsible for early growth inhibition under Mg deficiency in maize,” was rejected.

4.3 Reduced cell division in growing sink tissue is responsible for early growth inhibition of maize under Mg deficiency

Plant growth is realized by cell division and cell extension. Since the assimilates were in the same concentration range under Mg deficiency as in the control treatment, cell division was not limited by sugars or protein availability (see above). As an important parameter for cell division, DNA contents of leaves, roots, and root tips were determined. Magnesium is essential for the function of DNA polymerase (Stout and Arens, 1970). Therefore, Mg deficiency could result in a lower number of DNA present in the analyzed tissue. Since DNA replication is required for cell division, a lower DNA content would mean a lower number of cells. Throughout the experiment, Mg deficiency did not permanently affect DNA contents of the growing tissues (Figure 14), indicating that Mg as a cofactor for DNA polymerases did not limit cell division (Stout and Arens, 1970; Yang et al., 2004). Especially, when the growth rate was reduced in leaf 4, there was no difference in DNA content (Figure 9). Niu et al. (2015) did not find a reduction of meristematic cell numbers of root tissue in *Arabidopsis* grown under Mg deficiency, either. In conclusion, cell division of

growing leaves and root tips was not sensitive to Mg deficiency. Therefore, the hypothesis that “reduced cell division in growing sink tissue is responsible for early growth inhibition of maize under Mg deficiency,” was rejected. Since leaf growth was affected by Mg deficiency the other growth process, cell extension, must have been inhibited.

4.4 Altered PM H⁺-ATPase activity is responsible for reduced leaf apoplastic acidification reducing extension growth under Mg deficiency in maize

Reduced apoplastic acidification limits extension growth.

Apparently, it was cell extension that significantly inhibited leaf-area development (Figure 9). According to the acid-growth theory apoplastic acidification is necessary to loosen cell-wall compounds (Figure 1; recently reviewed by Dünser and Kleine-Vehn, 2015). This process is the basis for the cell expansion driven by turgor pressure (Hager et al., 1971). In this study, it was shown for the first time that apoplastic pH was increased under Mg deficiency (Table 3). Some authors suggested a possible change in apoplastic acidification without having measured this parameter (Cakmak and Kirkby, 2008; Neuhaus et al., 2013; Jezek et al., 2015). An apoplastic pH increase occurred in leaf 4 for which a decrease in growth was detectable 1 d later (compare Table 3 and Figure 9). None of the other parameters discussed above were altered in any way or to any time point, which could explain the Mg deficiency-induced growth inhibition. Therefore, in accordance with the acid-growth theory the higher apoplastic pH inhibited cell-extension growth (Hager et al. 1971; Dünser and Kleine-Vehn 2015).

Altered PM H⁺-ATPase performance is responsible for reduced apoplastic acidification

The PM H⁺-ATPase is responsible for cell-wall acidification (Palmgren, 2001), which in turn has a direct effect on cell-extension growth. It was tested whether a reduction of total PM H⁺-ATPase protein abundance might be responsible for the observed increase in apoplastic pH. No difference in the abundance was found (Figure 16), ruling out a decrease in acidification induced by a lack of total protein abundance in the plasma membrane.

There are other possible factors influencing the PM H⁺-ATPase activity and ultimately the apoplastic acidification *in vivo*, besides posttranslational modifications of the enzyme (recently reviewed by Falhof et al., 2016). It was shown by Hanstein et al. (2011) that Mg is necessary as a co-factor of ATP to activate the maize plasma membrane H⁺-ATPase. If Mg is not present as a co-factor or present at lower concentrations than ATP, ATP itself causes a competitive inhibition of the H⁺-ATPase (Hanstein et al. 2011). Therefore, the behavior of the PM H⁺-ATPase was characterized *in vitro*. In this experiment, it was assumed that 5 mM Mg was an optimal concentration for PM H⁺-ATPase activity measurements, similar to the concentration expected *in vivo* for plants grown under optimal nutrient supply. Yazaki et al. (1988) estimated that 3.8 mM Mg-ATP were present in the cytoplasm of mung bean root tips *in vivo*. In contrast, a Mg assay concentration of 1 mM was chosen to reflect conditions found in the cytoplasm of plants during Mg deficiency.

The turnover number (K_t), which indicates the amount of Mg-ATP hydrolyzed per second by the catalytic center of PM H⁺-ATPase, was determined *in vitro* at 1 mM and 5 mM Mg. K_t was significantly lower when the Mg concentration was 1 mM compared to 5 mM Mg (Table 4). This was true for control and Mg-deficient leaves. The results on the one hand confirm the findings of

Hanstein et al. (2011) that if the ATP concentration is higher than the Mg concentration, Mg-free ATP acts as a competitive inhibitor for Mg-ATP, decreasing the PM H⁺-ATPase activity. On the other hand, they explain why a decrease of apoplastic acidification was found *in vivo* for maize leaves growing under Mg deficiency (Table 3). The lack of cytoplasmatic Mg probably caused a competitive inhibition of PM H⁺-ATPase by Mg-free ATP.

However, the PM H⁺-ATPase activity was also altered in vesicles from Mg-deficient plants compared to those from control plants when 5 mM Mg were present *in vitro* (Figure 15). A higher hydrolytic activity was found for vesicles isolated from Mg-deficient plants indicating an adaptation of the enzyme. This adaptation was confirmed by altered enzymatic constants (Table 4). K_r was higher for the Mg-deficiency treatment compared to the control, indicating a higher substrate turnover at the catalytic site of the enzyme. However, the K_m of the hydrolytic activity was higher at 5 mM Mg assay concentration compared to the same samples at 1 mM Mg in the assay in the control, while there was no significant difference in the Mg-deficiency treatment between 5 and 1 mM Mg assay concentrations. It is concluded that an adaptation of the PM H⁺-ATPase occurred during Mg deficiency, which increased the turnover of Mg-ATP at the catalytic site, while the affinity of the enzyme to its substrate (Mg-ATP) remained unchanged, regardless of the Mg assay concentrations.

This adaptation was also seen in the higher maximum pH gradient in vesicles isolated from Mg-deficient plants (Table 5). The maximum pH gradient is a parameter which can be achieved with a given abundance of proton pumps and describes the plant vesicles' H⁺ influx and H⁺ efflux in an equilibrium. Since the maximum pH gradient was higher in vesicles derived from the Mg-deficient

plants the composition of proton pumps must have been different from the composition of control vesicles (Table 5). The passive H⁺ transport rate (H⁺ efflux) were not altered in the Mg-deficiency treatment, indicating that the plasma membrane itself was not modified (Table 5). However, this adaption of the enzyme is only measurable at 5 mM Mg present in the *in vitro* assay. The hydrolytic activity *in vitro* measurements with just 1 mM Mg present in the assay suggests that this adaption was not sufficient *in vivo* since at these low Mg assay concentrations the hydrolytic activity was the same in vesicles derived from control and Mg-deficiency treatment (Table 4 and Figure 15). The *in vivo* measured higher apoplastic pH (Table 3) indicates that the adaptation in the Mg-deficiency treatment was not sufficient to maintain the *in vivo* pH gradient at the PM on the control level. A lack of available Mg as co-substrate *in vivo* probably caused a lower proton-pumping activity of the PM H⁺-ATPase, resulting in a lower PM pH gradient, lowering the apoplastic acidification (Table 3), which finally caused a reduction in leaf extension growth (Figure 9). In conclusion, the hypothesis that “altered PM H⁺-ATPase activity is responsible for reduced leaf apoplastic acidification reducing extension growth under Mg deficiency in maize,” was accepted.

Altered expression of PM H⁺-ATPase isoforms may be responsible for altered PM H⁺-ATPase activity

One explanation amongst others (e.g. posttranscriptional and posttranslational modifications, recently reviewed by Falhof et al., 2016) for the detected adaptation of the enzyme is the transcription of different PM H⁺-ATPase isoforms. It was shown by Palmgren and Christensen (1994) that different isoforms of *Arabidopsis thaliana* exhibited different hydrolytic and pumping characteristics when heterologously expressed in yeast. The differences in hydrolytic activity and maximum pH gradient in the Mg-deficiency treatment at high Mg assay concentrations compared to the control was measured, too (Figure 15 and Table 5). Therefore, it was checked whether the

relative RNA abundance of the H⁺-ATPase isoforms was different in the Mg-deficiency treatment compared to the control. A higher transcript abundance of the *MHA4* isoform was found, suggesting a role in adaptation to Mg deficiency (Figure 17). Neuhaus et al. (2013) also showed that H⁺-ATPase isoforms were differently transcribed in Mg-deficient bean plants compared to control conditions with sufficient Mg supply. They concluded, without showing data of H⁺-ATPase activity or apoplastic acidification, that the different isoform composition could have altered H⁺ pumping and apoplastic acidification.

In order to explain the adaptation of the enzyme activity (lower K_m and higher K_r) it was tested whether there were any mutations at the amino acid level when *MHA4* was compared to other PM H⁺-ATPase isoforms, including *AHA2* of *Arabidopsis thaliana*. Most regions of the PM H⁺-ATPase isoforms are highly conserved. Only one amino acid in proximity to the phosphorylation site and to the Mg²⁺-binding site of the enzyme was identified as a mutation, which led to an amino acid with different side-strain polarity in the protein. Here, the serine in *MHA2* of maize and in *AHA2* of *Arabidopsis* (amino acid position 445) was replaced by glycine in *MHA4*. However, a closer look at the 3D folding of the protein revealed that this mutation is located in the alpha helix on the opposite site of the nucleotide binding domain and points away from the Mg-ATP binding site (Pedersen et al., 2007). Given the relative lack of reactivity of the identified residues, in conjunction with the large distance from the Mg²⁺ binding site, it is highly unlikely that this mutation is responsible for the observed adaptation effect.

Another amino acid substitution in *MHA4* was found at amino acid number 895, where the neutral amino acids proline in *AHA2* (*Arabidopsis*) and asparagine in *MHA2* (maize) were exchanged against the basic amino acid histidine. This exchange took place in direct proximity to two phosphorylation sites (T881 and S899) in the R-domain of the PM H⁺-ATPase. Phosphorylation reactions at these sites were responsible for up- and down-regulation of H⁺ pumping activity

(Fuglsang et al., 2014; Haruta et al., 2015). An amino acid exchange in close proximity of these phosphorylation sites could influence the function of these sites with regard to changes in pumping activity. The basic nature of the histidine in *MHA4* may change the 3D structure and influence the phosphorylation site 881 compared to the neutral amino acid in *MHA2* and *AHA2*. Unfortunately, the exact 3D structure of *AHA2* of *Arabidopsis thaliana* of this region (844 to 899) is unknown (Pedersen et al. 2007). Consequently, the hypothesis that an exchange of a neutral against a basic amino acid in *MHA4* at site 895 enabled active adaptation found in the hydrolytic activity under Mg deficiency remains pure speculation. It is concluded that the main parts of the PM H⁺-ATPase are highly conserved, regardless of the expressed isoforms. Therefore, the differential abundance of the isoform *MHA4* probably does not explain the adaptation of the enzyme under Mg deficiency observed in the kinetic parameters.

4.5 Source leaf sugar supply limits maize kernel development under salt stress

Salt stress reduced the kernel number in both genotypes (Figure 19 B). However, the reduction was stronger for Pioneer 3906 than for Fabregas, which is in line with the results of a previous study (Hütsch et al., 2015) that was conducted under similar experimental conditions in the years 2011 and 2012. A reduction in kernel number is often observed when maize is subjected to abiotic stress. Kernel development is often terminated in a timeframe of just a few days after pollination. Especially kernels at the apical end of cobs are susceptible to kernel abortion and abiotic stress can increase the number of aborted kernels (Oury et al., 2015). Therefore, the physiological causes for kernel abortion at 0 and 2 DAP under salt stress were investigated.

A reduction in kernel FW was found in the developing kernels 2 DAP in 2012 (Hütsch et al., 2015) and also in the present experiment (Figure 21 B). The reduction of the kernels FW is the first indicator for the observed number of aborted kernels at maturity (Figure 19 B and Figure 21 B). Sucrose and hexoses accumulated in the kernel tissue in both years 2 DAP (Hütsch et al. 2015 and Figure 23). The higher sucrose concentrations in the sink tissue (Figure 23 C) along with just a slight decrease in transpiration rate in the experiments 2011 and 2012 (Hütsch et al., 2015) and 2014 (data not shown) suggest that assimilate supply was not limited. While overall photosynthesis is often reduced under salt stress, this reduction seldom impairs photoassimilate availability in sink tissues (Ruan et al., 2012; Henry et al., 2015; Hütsch et al., 2015; Hütsch et al., 2016). Since there was no limitation in photoassimilate supply, source limitation can be ruled out as a reason for early kernel abortion. Therefore, the hypothesis that “source leaf sugar supply limits maize kernel development under salt stress,” was rejected.

4.6 Sink hexose supply limits maize kernel development under salt stress

The unimpaired hexose supply of the kernels is a necessity for kernel development. The endosperm undergoes a period of very rapid cell division and cell elongation during the first 12 DAP (Scanlon and Takacs, 2009). The cell's energy status has to be in an optimal range for both growth processes to work properly. Hexoses are the fuel for ATP synthesis which is the universal energy source for metabolism. The sinks are entirely dependent on sugar supply from source leaves during the first days after fertilization (Bihmidine et al., 2013). Since source limitation can be excluded (see above), a limitation in the sink tissue is probably the reason for kernel starvation. The high hexose concentrations (Figure 23 A, B) demonstrate that the sugars were not metabolized in the growing tissue. Either metabolic processes in the cytoplasm of kernels were inhibited under salinity, or the

hexoses resulting from acid invertase catalyzed hydrolysis of sucrose (Figure 25) remained in the apoplast and were not transported into the cytoplasm (Figure 23). Henry et al. (2015) also found an accumulation of sucrose and hexoses in kernel tissue 3 DAP under salt stress. They also found lower concentrations of citric acid cycle intermediates in this tissue and concluded that respiration in the kernels was impaired, indicating a low energy status. Astonishingly, the kernel fresh weight increased in the salt stress treatment under their experimental conditions at 0 and 3 DAP.

The transport of hexoses through the plasma membrane is most likely conducted by hexose carriers (Hütsch et al., 2015) powered by the pH gradient at the PM membrane (Sondergaard et al., 2004). The transport by carriers is the main way of sugar transport into the kernel daughter cells, since there is no symplastic continuum by plasmodesmata between maternal kernel cells and daughter kernel cells (Bihmidine et al., 2013). The pH gradient is built up by the PM H⁺-ATPase (Zhao et al., 2000) and the ATPase is activated e.g. by high sugar concentrations, which mediates the binding of 14-3-3 proteins to the regulatory (R-) domain (Okumura et al., 2016). It has been shown previously that the PM H⁺-ATPase activity is lower under salt stress in shoot tissue of maize in the vegetative stage. In these studies the lower PM H⁺-ATPase activity often caused a reduction in apoplastic acidification (Zörb et al., 2005b; Hatzig et al., 2010), which means that the pH gradient at the PM was reduced. However, no study is known in which the activity of PM H⁺-ATPase was assessed in developing kernels under salt stress. In conclusion, the hypothesis that “sink hexose supply limits maize kernel development under salt stress,” was accepted.

4.7 Plasma membrane H⁺-ATPase activity of young maize kernels is reduced under salt stress, inhibiting hexose uptake of the sink tissue, leading to kernel starvation

The results show that in the analyzed kernel tissue the *in vitro* PM H⁺-ATPase activity was altered in the salt stress treatment (Table 6). The hydrolytic activity was significantly reduced for both genotypes 2 DAP, while there was no difference in hydrolytic activity just before pollination (0 DAP) for Pioneer 3906 and even an increase in hydrolytic activity in the case of Fabregas (Table 6 and Figure 26). The maximum pH gradient was reduced in Pioneer 3906 2 DAP in the salt stress treatment (Table 7). The maximum pH gradient is influenced by active H⁺ transport rate (H⁺ influx) and the passive H⁺ transport rate (H⁺ efflux) which is a parameter to characterize the proton leakage of the PM. Since neither H⁺ transport rate nor the passive H⁺ transport rate were altered, there has to be another factor involved.

The composition of isoforms of the PM H⁺-ATPase can also have a significant influence on the pH gradient, since some isoforms are more efficient in proton pumping than others (Palmgren and Christensen, 1994). However, no difference in the expression pattern at the RNA level was found between Pioneer 3906 control and Pioneer salt stress 2 DAP (Figure 27). Yet, the only other factor that could explain the difference in the maximum pH gradient is the total protein abundance of the PM H⁺-ATPase, which was lower in the salt stress treatment compared to the control (Figure 28). This indicates that a lower number of proton pumps were present in the kernel PM of the salt stress treatment at this point after fertilization. Since the composition transcripts of the PM H⁺-ATPase isoforms apparently did not change (Figure 27), the lower total abundance of PM H⁺-ATPases in pioneer 3906 (Figure 28) was responsible for the reduced maximal pH gradient (Table 7). In the same treatment, there were also a lower hydrolytic activity (Figure 26) and a lower K_r (Table 6).

The lower number of PM H⁺-ATPases present in the PM also means a lower number of Mg-ATP binding sites, which explains the measured lower turnover rate (K_t) of the substrate Mg-ATP.

In conclusion, the hexose uptake into the endosperm was most likely reduced due to a lower pH gradient energizing the hexose transport (Sondergaard et al., 2004). The lower hexose availability in endosperm and embryo probably caused kernel abortion, which resulted in the reduction of kernel number at maturity (Figure 19 B, Figure 20). The decrease in kernel number in the salt stress treatment was more severe for Pioneer 3906 (-34%) than for Fabregas (-19%) (Figure 19 B, Figure 20). For Fabregas just a slight reduction of the PM H⁺-ATPase hydrolytic activity was found (Figure 26 B), along with a small significant reduction in the relative RNA abundance of some PM H⁺-ATPase isoforms. The other parameters to characterize the PM H⁺-ATPase performance were not as negatively affected as they were in Pioneer 3906. The smaller impact of salt stress on the PM H⁺-ATPase activity may explain the lower number of aborted kernels in Fabregas.

The hexose concentrations were higher in the salt stress treatment just prior to pollination (0 DAP) in both genotypes, too (Figure 23 A, B). However, at this harvest date, no lower *in vitro* PM H⁺-ATPase activity (Table 6 and Table 7) was detectable and no reduction in kernel fresh weight, either (Figure 21 B). The PM H⁺-ATPase pumping activity is tightly controlled by posttranscriptional modifications (recently reviewed by Falhof et al., 2016) which could be responsible for changes in the PM H⁺-ATPase activity *in vivo*, which were not measurable *in vitro*.

However, besides hexose concentrations, sucrose concentrations were increased 0 DAP, too. They were even more elevated 0 DAP than 2 DAP at least in Pioneer 3906 (Figure 23). This accumulation suggests, that maybe another growth process was inhibited by a lack of hexose uptake already at 0 DAP. The investigated kernel tissue is not the only sink tissue on the cobs, that was still developing 0 DAP and has no viable symplastic connection to the rest of the plant to transport photoassimilates. The silks belong to the daughter cell tissue of the kernel (Figure 4), like embryo and endosperm (Bedinger and Fowler, 2009). Every single kernel has an elongated stigma (the silks) that originates near the embryo and grows from there out of the husk leaves till it reaches its final size or gets pollinated. Since it is growing quite fast (approximately 3.8 cm d^{-1}), nearly exclusively by cell extension growth, the silk cells have a high demand for hexoses for metabolism, too. The silk fresh weight was reduced on the day of pollination in the salt-stress treatment, indicating that the growth process was inhibited (Figure 22). Oury et al. (2016) studied the reduction of silk elongation rates and fresh weight under drought stress. Under drought stress they found a reduced upregulation at the transcript level of enzymes for cell-wall modifying enzymes that are involved in cell-extension growth.

Since the kernel development in the first phase of salt stress is similar to the development during drought stress (Hütsch et al., 2015) it could be hypothesized that a similar modification also occurred in the present experiment. Oury et al. (2016) also found an accumulation of sugars in the kernel tissue along with a reduced acid invertase activity 0 DAP, and no reduction in kernel growth, (compare Figure 21 B, Figure 23, and Figure 25). There seem to be many similarities between the effect of drought stress and salt stress of the first phase on maize silk development. Future studies should address this and focus on the reasons for reduced silk extension growth. Since the

accumulation of sugars at 0 DAP in the kernel tissue hints to a similar reason for growth reduction for silks as for the kernels 2 DAP, the hexose concentration of silks should be analyzed separately. In addition, it is not unreasonable to speculate that the PM H⁺-ATPase also plays a major role in growth reduction of silks by means of reduced apoplastic acidification. In conclusion, the hypothesis that “plasma membrane H⁺-ATPase activity of young maize kernels is reduced under salt stress, inhibiting hexose uptake of the sink tissue, leading to kernel starvation,” was accepted.

5. Conclusions

This thesis shows that under both environmental constrains (Mg deficiency and salt stress) the PM H⁺-ATPase plays a major role in the plants' response towards these abiotic stresses.

5.1 Reduced PM H⁺-ATPase activity limits cell-extension growth under Mg deficiency in maize

Magnesium is involved in a number of physiological processes that determine plant growth. It was demonstrated for the first time that reduced apoplastic acidification primarily limits plant growth under Mg deficiency.

The plant firstly reacts to Mg deficiency with an increase of the relative RNA abundance of the PM H⁺-ATPase isoform *MHA4* (Figure 17). This increased the PM H⁺-ATPase activity *in vitro* compared to control under high Mg assay concentrations (5 mM), implicating an adaption of the enzyme (Table 5). This adaptation was not sufficient to maintain apoplastic acidification under low Mg concentrations *in vivo*: A lack of Mg as a co-substrate for PM H⁺-ATPase inhibited its activity, which measurably reduced apoplastic acidification regardless of the enzyme adaptation (Table 4 and Table 5). This resulted finally in reduced extension growth of maize leaves under Mg deficiency (Figure 9). The sequential physiological responses of maize to Mg deficiency are summarized in Figure 29.

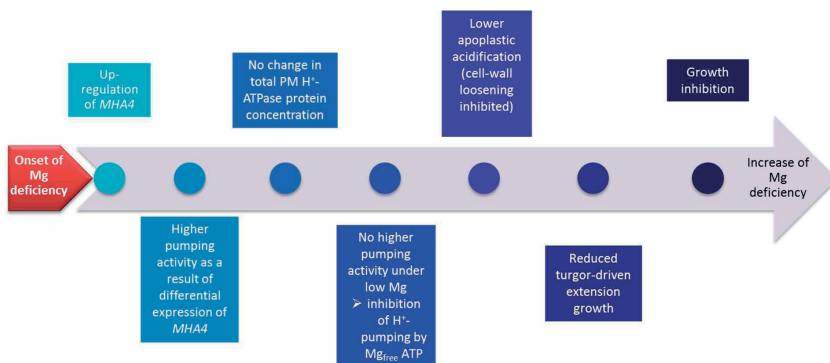


Figure 29: Proposed mechanism for reduced growth under Mg deficiency in young maize plants.

The lower apoplastic acidification (Table 3) is the reason for the initial growth inhibition of maize under Mg deficiency. However, as the severity of Mg deficiency increases with further growth other physiological factors may limit the development of the plant even further. In this thesis and in other studies a strong accumulation of sugars was observed in the mature source leaves (Figure 12 and Cakmak et al., 1994b; Fischer et al., 1998; Hermans et al., 2004b; Mengutay et al., 2013). These accumulated sugars are potentially missing for the metabolic processes of sink tissues in other parts of older plants. Since the accumulation gets more severe over time, sooner or later, the sink tissues will be subjected to a source limitation by a lack of photoassimilates. Some authors (e.g. Cakmak et al., 1994a; Neuhaus et al., 2013) suggested that a decrease of PM H⁺-ATPase activity could be responsible for an inhibited phloem transport of sucrose from leaf source tissue to sink tissues. Since sucrose is mainly loaded into the phloem by means of sucrose/H⁺ cotransporters, a lower pH gradient would reduce the transport rate of sucrose (Sondergaard et al., 2004). However, this hypothesis has not been tested yet and should be tested in future studies.

5.2 Reduced PM H⁺-ATPase activity limits maize kernel sugar uptake under salt stress

It was shown for the first time that young maize kernel PM H⁺-ATPase activity is negatively affected under salt stress, probably playing a key role in kernel abortion under these environmental constraints.

In contrast to shoot growth, kernel growth was not inhibited by salt stress till fertilization (Figure 21 B, C). The first reduction of kernel development occurred in the timeframe between the pollination of silks and the next harvest 2 d later. It takes a maximum of 24 h from the pollination of silks till the fertilization of the ovule. In the first days after fertilization rapid cell division and extension growth takes place in the endosperm and the embryo (Bihmidine et al., 2013). The cells of these tissues need hexoses to energize the underlying physiological processes. However, salt stress inhibited kernel growth 2 DAP (Figure 21 B), while sugars accumulated at the same time in kernel tissue (Figure 23). Plasma membrane H⁺-ATPase activity was only impaired 2 DAP (Table 7 and Figure 26) when kernel growth was reduced, but not 0 DAP when growth was not reduced (Figure 21 B). The pH gradient across the PM is important to energize hexose transporters which are also localized in the PM. Since this pH gradient was reduced under the salt stress treatment, it is assumed that due to the reduced energization of hexose transporters, a lower amount of hexoses was transported into the daughter cells. This resulted in an accumulation of sugars in the whole kernel (Figure 23) and in a lower hexose availability for the biochemical processes in the cytoplasm of daughter cells. The lower availability of hexoses in the cytoplasm of endosperm and embryo probably limited cell division and extension, which caused the reduced kernel growth. This proposed chain of events is summarized in Figure 30.

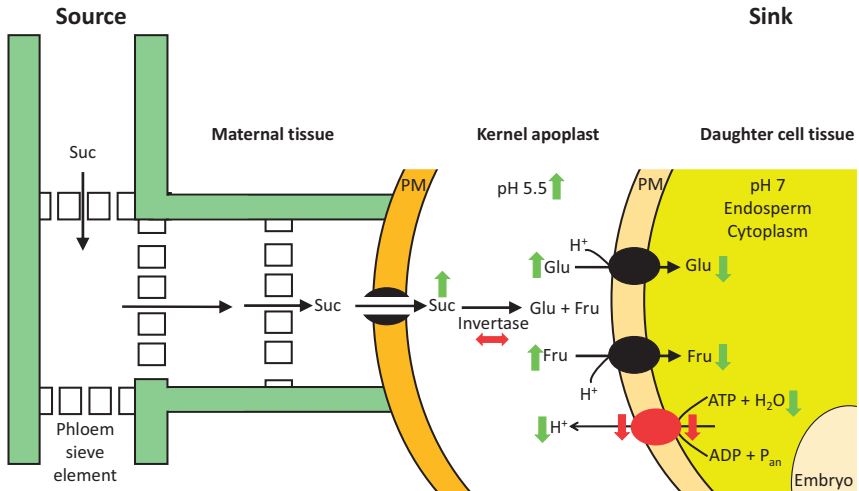


Figure 30: Sucrose (Suc) transport from source (leaves) to the sink (kernels) of maize. Suc moves through the phloem to the sink where it is released non-selectively through the plasma membrane (orange). In the kernels apoplast it is hydrolyzed by means of acid invertase to Glucose (Glu) and Fructose (Fru). The daughter cells take up Glu and Fru selectively with hexose transporters (black). The transporters are energized with the pH gradient, established by the PM H⁺-ATPase (red). Green arrows indicate measured changes of processes; red arrows indicate proposed changes of processes (Partly redrawn after Tang and Boyer, 2013).

Previously, it has been shown that auxin plays an important role in PM H⁺-ATPase activity, apoplastic pH decrease, and cell-extension growth of developing maize kernels. Indole-3-acetic acid (IAA) activates the PM H⁺-ATPase and determines the extent of apoplastic acidification and cell-extension growth (Rober-Kleber et al., 2003). Furthermore, it has been shown that cell wall invertase-deficient maize kernels produced lower concentrations of IAA (LeClere et al., 2010). In this experiment the hexose concentrations were lower in the *mn1* (miniature1) mutant kernels compared to wild-type kernels. Therefore, it can be assumed that cell-wall invertase activity and auxin synthesis are positively correlated. Additionally, differences in IAA and IBA (indole-3-

butyric acid) concentrations in vegetative maize plant tissue (shoot and root) were observed under salt stress. The degree of altered auxin concentration seemed to be correlated with the degree of salt resistance of two maize genotypes (Zörb et al., 2013).

Therefore, there is a possible link between cell-wall invertase activity, the concentration of hexoses and auxin production on the one hand, and PM H⁺-ATPase activity, apoplastic acidification and cell-extension growth on the other hand. Regrettably, these parameters have not yet been investigated together. In the present thesis, the auxin concentrations were not determined, hence in future studies all mentioned parameters should be measured regarding maize kernel development under abiotic stress. Especially, since it was already shown that the salt-resistant genotype SR03 can maintain or even increase auxin concentrations in its vegetative tissue as well as apoplastic acidification and extension growth compared to salt sensitive genotypes (Zörb et al., 2013).

5.3 Contribution of the PM H⁺-ATPase to physiological responses under abiotic stress differs depending on plant organ

The establishment of an electrochemical gradient by pumping protons from the cytoplasm into the apoplast has two main functions:

The acidification of the cell wall as a prerequisite for cell extension growth and the energization of transport processes of symporters and antiporters at the PM (Sondergaard et al., 2004). The importance of these main functions differ under abiotic stress, depending on the affected tissue.

1. In growing vegetative leaf sink tissue, the reduced apoplastic acidification is the main problem for the plant under abiotic stress. There is a symplastic continuum which connects

autotrophic source leaves and heterotrophic sink leaves, making symplastic transport the preferred transport route for photoassimilates to leaf sink tissue (Hütsch et al., 2016). Thus, unloading of sucrose from the phloem via the apoplastic pathway is negligible, reducing the importance of the PM H^+ -ATPase to build up a pH gradient for the energization of carrier-mediated hexose uptake. Since the hexose concentrations were not reduced in growing leaves (Figure 12), but apoplastic acidification (Table 3) and leaf extension growth (Figure 9) was reduced under Mg deficiency, not a lack of photoassimilates reduced cell-extension growth, but a lack of apoplastic acidification.

2. The situation is different for generative kernel tissue. Here, the main problem for the plant is the impaired establishment of the pH gradient for the energization of transport processes. There is no symplastic continuum between autotrophic source leaves and heterotrophic tissue of daughter cells in the kernels. Therefore, the apoplastic pathway is mandatory for the transport of photoassimilates (Bihmidine et al., 2013). An accumulation of sugars was found in the tissue of the whole kernels in the salt-stress treatment (Figure 23) indicating that this apoplastic route was partly blocked. The blockade was probably caused by a reduced pH gradient across the PM (Table 7). Here, the proper establishment of a pH gradient for the energization of transport processes with carriers for hexose uptake is obligatory. The lower pH gradient presumably reduced the hexose uptake, which probably resulted in a reduced energy status of the cells in the daughter tissue. The lower energy status supposedly inhibited cell division which resulted in the measured reduced kernel growth (Figure 21 B) 2 DAP and a reduced number of kernels at maturity (Figure 19 B and Figure 20).

6. Summary

The plasma membrane (PM) H^+ -ATPase is the powerhouse of the plant. The enzyme establishes an electrochemical proton gradient across the PM. This gradient is responsible for cell-wall acidification which is a requisite for cell-extension growth and it energizes transport processes of symporters and antiporters at the PM. Abiotic stresses often have a negative impact on the functions of enzymes which can disturb major physiological processes and interfere with plant development. Therefore, the effect of abiotic stress on the PM H^+ -ATPase's two main functions were investigated in this thesis. The effect of Mg deficiency on apoplastic acidification was studied in developing maize leaves and the effect of salt stress on energization of transport processes was examined in developing maize kernels.

Magnesium (Mg) deficiency is often observed in agricultural crops with an insufficient Mg fertilization regime, finally resulting in yield depression. One goal was to identify the process that primarily limits maize (*Zea mays* L.) growth and yield under insufficient Mg supply. A sufficient (500 μ M) and a low (25 μ M) Mg concentration were used in time-course hydroponic experiments to investigate parameters which are considered to be important for the characterization of the key processes of growth, namely cell division and cell-extension growth. It was shown that cell division was not susceptible to Mg deficiency, since neither DNA replication nor sugar or protein availability limited this growth process. However, PM H^+ -ATPase activity was inhibited by a lack of the enzyme's co-substrate Mg under Mg deficiency. The inhibition of the PM H^+ -ATPase reduced apoplastic acidification causing a reduced cell-extension growth. This primarily limited maize growth under Mg deficiency.

Salt stress affects yield formation of maize at various physiological levels resulting in an overall decrease of grain yield. In this thesis it was investigated how salt stress affects kernel development at and shortly after pollination. Maize kernels grown under control and salt stress were harvested 0 and 2 d after pollination (DAP) and at kernel maturity. Kernel development was not inhibited 0 DAP, but it was inhibited 2 DAP under salt stress. On this day, kernel PM H⁺-ATPase activity was reduced which caused a lower pH gradient across the plasma membranes of endosperm and embryo tissue. The lower pH gradient supposedly resulted in a decreased energization of transporters responsible for hexose import into the cytoplasm of the kernels. A lack of hexoses reduced the energy status of the cells which impaired cell division. The impaired cell division probably caused the observed growth reduction of kernels 2 DAP, which resulted in an observed lower kernel number and grain yield at maize maturity under salt stress.

It is concluded that the impairment of PM H⁺-ATPase by Mg deficiency and salt stress in maize is a major reason for growth and yield reduction under these environmental constraints. However, while the impairment of the cell-wall acidification is the reason for a reduced extension growth under Mg deficiency in leaves, the decrease in pH gradient at the PM caused kernel abortion under salt stress.

7. Zusammenfassung

Die Plasmamembran (PM) H^+ -ATPase wird aufgrund ihrer herausragenden Stellung im pflanzlichen Stoffwechsel als Kraftwerk oder als Masterenzym der Pflanze bezeichnet. Sie baut an der Plasmamembran pflanzlicher Zellen einen elektrochemischen Protonengradienten auf, der zweierlei Funktionen hat: 1. Die Ansäuerung der pflanzlichen Zellwand, welches die Voraussetzung für die Turgor-getriebene Zellstreckung ist. 2. Den Antrieb von Transportprozessen durch die Plasmamembran.

Abiotischer Stress hat oft einen negativen Einfluss auf diese Funktionen. Eine Störung einer dieser beiden Funktionen hat oft negative Einflüsse auf wichtige physiologische Prozesse, wodurch wiederum die normale Entwicklung der Pflanze gestört werden kann. Daher wurde in dieser Arbeit untersucht, welche Auswirkungen abiotischer Stress auf die beiden Funktionen des pH-Gradienten hat. Der Einfluss von Magnesiummangel auf die Ansäuerung des Apoplasten wurde in noch wachsenden Maisblättern untersucht, während in sich entwickelnden Maiskörnern der Einfluss von Salzstress auf den Antrieb von Transportprozessen in der PM untersucht wurde.

In landwirtschaftlichen Kulturen wird häufig Magnesiummangel aufgrund einer unzureichenden Magnesiumdüngung beobachtet, welcher zu einem reduzierten Ertrag führen kann. Ein Ziel dieser Arbeit war es daher, den Prozess zu identifizieren, der unter Magnesiummangel primär das Wachstum und den Ertrag von Mais (*Zea mays* L.) reduziert. Mit einer niedrigen (25 μ M) und einer hohen Magnesiumkonzentration (500 μ M) wurden daher Nährlösungsversuche durchgeführt, um

Parameter für die physiologischen Wachstumsprozesse wie Zellteilung und Zellstreckung zu erfassen. Es konnte gezeigt werden, dass die Zellteilung weder durch die DNA-Replikation noch durch die Verfügbarkeit von Zuckern oder Proteinen negativ durch Magnesiummangel beeinflusst wurde. Jedoch war unter Magnesiummangel die Aktivität der PM H⁺-ATPase durch einen Mangel an dem für das Enzym notwendigen Co-Substrats Magnesium reduziert. Durch die Hemmung der Aktivität der PM H⁺-ATPase unter Magnesiummangel konnte die Ansäuerung des Apoplasten nicht aufrechterhalten werden, sodass hierdurch das Zellstreckungswachstum eingeschränkt wurde. Dies war der primäre Grund für das reduzierte Wachstum von Mais unter Magnesiummangel.

Salzstress behindert die Ertragsbildung von Mais auf verschiedenen physiologischen Ebenen, was schließlich zu einem verminderten Ertrag führt. In dieser Arbeit wurde daher untersucht, welche Auswirkungen Salzstress auf die Entwicklung von jungen Maiskörnern während oder kurz nach der Bestäubung hat. Hierzu wurde Mais unter Kontrollbedingungen und unter Salzstress angebaut und die Körner am Tag der Bestäubung, zwei Tage später und zur Kornreife geerntet. Das Wachstum der Körner war zum Zeitpunkt der Bestäubung noch nicht durch den Salzstress reduziert, jedoch zwei Tage später schon. An diesem Tag wurde eine Reduktion der Aktivität der PM H⁺-ATPase gemessen, die einen reduzierten pH-Gradienten an den Plasmamembranen von Endosperm und Embryo zur Folge hatte. Diese Reduktion verursachte wahrscheinlich einen reduzierten Transport von Hexosen in das Cytoplasma der Körner. Der Mangel an Hexosen im Cytoplasma rief mutmaßlich einen verringerten Energiestatus der Zelle hervor, der in einer verringerten Zellteilung resultierte. Dies war vermutlich die Ursache für die beobachtete

Wachstumsreduktion der Körner zwei Tage nach der Bestäubung. Dies mündete in eine verminderte Anzahl von Körnern und in einen verringerten Ertrag bei der Kornreife.

Es bleibt festzuhalten, dass die Reduzierung der Aktivität PM H^+ -ATPase durch Magnesiummangel und Salzstress ein Hauptgrund für vermindertes Wachstum und Ertragsdepression war. Die reduzierte Ansäuerung des Apoplasten war der Grund für das reduzierte Streckungswachstum der Blätter unter Magnesiummangel, während der reduzierte pH-Gradient an der Plasmamembran unter Salzstress das Absterben der Körner verursachte.

8. References

- Bedinger PA, Fowler JE** (2009) The Maize Male Gametophyte. *In* JL Bennetzen, SC Hake, eds, *Handb. Maize Its Biol.* Springer New York, pp 57–77
- Bhimidine S, Hunter CTI, Johns CE, Koch KE, Braun DM** (2013) Regulation of assimilate import into sink organs: update on molecular drivers of sink strength. *Plant Physiol* **4**: 177
- Bogoslavsky L, Neumann PM** (1998) Rapid regulation by acid pH of cell wall adjustment and leaf growth in maize plants responding to reversal of water stress. *Plant Physiol* **118**: 701–709
- Borrás L, Westgate ME, Otegui ME** (2003) Control of kernel weight and kernel water relations by post-flowering source–sink ratio in maize. *Ann Bot* **91**: 857–867
- Boyer JS** (1982) Plant productivity and environment. *Science* **218**: 443–448
- Bradford MM** (1976) A rapid and sensitive method for the quantitation of microgram quantities of protein utilizing the principle of protein-dye binding. *Anal Biochem* **72**: 248–254
- Briskin DP, Poole RJ** (1983) Characterization of a K⁺-stimulated adenosine triphosphatase associated with the plasma membrane of red beet. *Plant Physiol* **71**: 350–355
- Bullock DG, Anderson DS** (1998) Evaluation of the Minolta SPAD-502 chlorophyll meter for nitrogen management in corn. *J Plant Nutr* **21**: 741–755
- Cakmak I, Hengeler C, Marschner H** (1994a) Changes in phloem export of sucrose in leaves in response to phosphorus, potassium and magnesium deficiency in bean plants. *J Exp Bot* **45**: 1251–1257
- Cakmak I, Hengeler C, Marschner H** (1994b) Partitioning of shoot and root dry matter and carbohydrates in bean plants suffering from phosphorus, potassium and magnesium deficiency. *J Exp Bot* **45**: 1245–1250
- Cakmak I, Kirkby EA** (2008) Role of magnesium in carbon partitioning and alleviating photooxidative damage. *Physiol Plant* **133**: 692–704
- Cramer GR, Urano K, Delrot S, Pezzotti M, Shinozaki K** (2011) Effects of abiotic stress on plants: a systems biology perspective. *BMC Plant Biol* **11**: 163
- De Michelis MI, Spanswick RM** (1986) H⁺-pumping driven by the vanadate-sensitive ATPase in membrane vesicles from corn roots. *Plant Physiol* **81**: 542–547
- Dünser K, Kleine-Vehn J** (2015) Differential growth regulation in plants - the acid growth balloon theory. *Curr Opin Plant Biol* **28**: 55–59
- Falhof J, Pedersen JT, Fuglsang AT, Palmgren M** (2016) Plasma membrane H⁺-ATPase regulation in the center of plant physiology. *Mol Plant* **9**: 323–337

- FAO** Statistical Pocketbook 2015. Food Agric. Organ. U. N., <http://www.fao.org/documents/card/en/c/383d384a-28e6-47b3-a1a2-2496a9e017b2>
- Fischer ES, Lohaus G, Heineke D, Heldt HW** (1998) Magnesium deficiency results in accumulation of carbohydrates and amino acids in source and sink leaves of spinach. *Physiol Plant* **102**: 16–20
- Fortmeier R, Schubert S** (1995) Salt tolerance of maize (*Zea mays* L.): the role of sodium exclusion. *Plant Cell Environ* **18**: 1041–1047
- Fuglsang AT, Kristensen A, Cuin TA, Schulze WX, Persson J, Thuesen KH, Ytting CK, Oehlenschläger CB, Mahmood K, Sondergaard TE, et al** (2014) Receptor kinase-mediated control of primary active proton pumping at the plasma membrane. *Plant J Cell Mol Biol* **80**: 951–964
- Gallagher SR, Leonard RT** (1982) Effect of vanadate, molybdate, and azide on membrane-associated ATPase and soluble phosphatase activities of corn roots. *Plant Physiol* **70**: 1335–1340
- Galtier N, Belver A, Gibrat R, Grouzis JP, Rigaud J, Grignon C** (1988) Preparation of corn root plasmalemma with low Mg-ATPase latency and high electrogenic H pumping activity after phase partitioning. *Plant Physiol* **87**: 491–497
- Gévaudant F, Duby G, von Stedingk E, Zhao R, Morsomme P, Boutry M** (2007) Expression of a constitutively activated plasma membrane H⁺-ATPase alters plant development and increases salt tolerance. *Plant Physiol* **144**: 1763–1776
- Guo W, Nazim H, Liang Z, Yang D** (2016) Magnesium deficiency in plants: An urgent problem. *Crop J* **4**: 83–91
- Hager A, Menzel H, Krauss A** (1971) Versuche und Hypothese zur Primärwirkung des Auxins beim Streckungswachstum. *Planta* **100**: 47–75
- Hanstein S, Wang X, Qian X, Friedhoff P, Fatima A, Shan Y, Feng K, Schubert S** (2011) Changes in cytosolic Mg²⁺ levels can regulate the activity of the plasma membrane H⁺-ATPase in maize. *Biochem J* **435**: 93–101
- Haruta M, Gray WM, Sussman MR** (2015) Regulation of the plasma membrane proton pump (H⁺-ATPase) by phosphorylation. *Curr Opin Plant Biol* **28**: 68–75
- Hatzig S, Hanstein S, Schubert S** (2010) Apoplast acidification is not a necessary determinant for the resistance of maize in the first phase of salt stress. *J Plant Nutr Soil Sci* **173**: 559–562
- Hawkesford M, Horst W, Kichey T, Lambers H, Schjoerring J, Möller IS, White P** (2012) Chapter 6 - Functions of Macronutrients. *In* P Marschner, ed, *Marschners Miner. Nutr. High. Plants Third Ed.* Academic Press, San Diego, pp 135–189

- Henry C, Bledsoe SW, Griffiths CA, Kollman A, Paul MJ, Sakr S, Lagrimini LM** (2015) Differential Role for Trehalose Metabolism in Salt-Stressed Maize. *Plant Physiol* **169**: 1072–1089
- Hermans C, Bourgis F, Faucher M, Strasser RJ, Delrot S, Verbruggen N** (2004a) Magnesium deficiency in sugar beets alters sugar partitioning and phloem loading in young mature leaves. *Planta* **220**: 541–549
- Hermans C, Conn SJ, Chen J, Xiao Q, Verbruggen N** (2013) An update on magnesium homeostasis mechanisms in plants. *Metallomics* **5**: 1170–1183
- Hermans C, Johnson GN, Strasser RJ, Verbruggen N** (2004b) Physiological characterisation of magnesium deficiency in sugar beet: acclimation to low magnesium differentially affects photosystems I and II. *Planta* **220**: 344–355
- Hermans C, Verbruggen N** (2005) Physiological characterization of Mg deficiency in *Arabidopsis thaliana*. *J Exp Bot* **56**: 2153–2161
- Hörtensteiner S, Kräutler B** (2011) Chlorophyll breakdown in higher plants. *Biochim Biophys Acta BBA - Bioenerg* **1807**: 977–988
- Hütsch BW, Jung S, Schubert S** (2015) Comparison of salt and drought-stress effects on maize growth and yield formation with regard to acid invertase activity in the kernels. *J Agron Crop Sci* **201**: 353–367
- Hütsch BW, Osthusenrich T, Faust F, Kumar A, Schubert S** (2016) Reduced sink activity in growing shoot tissues of maize under salt stress of the first phase may be compensated by increased PEP-carboxylase activity. *J Agron Crop Sci* doi: 10.1111/jac.12162
- Hütsch BW, Saqib M, Osthusenrich T, Schubert S** (2014) Invertase activity limits grain yield of maize under salt stress. *J Plant Nutr Soil Sci* **177**: 278–286
- Jackson D** (2009) Vegetative Shoot Meristems. In JL Bennetzen, SC Hake, eds, *Handb. Maize Its Biol*. Springer New York, pp 1–12
- Jezek M, Geilfus C-M, Mühlhling K-H** (2015) Glutamine synthetase activity in leaves of *Zea mays* L. as influenced by magnesium status. *Planta* 1–11
- Kiss SA** (1988) Effect of magnesium on juvenility and rejuvenescence of plant cells, and its possible mechanism. *Magnes Res* **1**: 177–183
- Kobayashi NI, Tanoi K** (2015) Critical issues in the study of magnesium transport systems and magnesium deficiency symptoms in plants. *Int J Mol Sci* **16**: 23076–23093
- Koning LA, Veste M, Freese D, Lebzien S** (2015) Effects of nitrogen and phosphate fertilization on leaf nutrient content, photosynthesis, and growth of the novel bioenergy crop *Fallopia sachalinensis* cv. “Igniscum Candy.” *J Appl Bot Food Qual* **88**: 22–28

- Kräutler B** (2008) Chlorophyll breakdown and chlorophyll catabolites in leaves and fruit. *Photochem Photobiol Sci* **7**: 1114–1120
- Kuzmič P** (1996) Program DYNAFIT for the analysis of enzyme kinetic data: application to HIV proteinase. *Anal Biochem* **237**: 260–273
- LeClere S, Schmelz EA, Chourey PS** (2010) Sugar levels regulate tryptophan-dependent auxin biosynthesis in developing maize kernels. *Plant Physiol* **153**: 306–318
- Lorenzen CJ** (1967) Determination of chlorophyll and phaeo-pigments: Spectrophotometric equations. *Limnol Oceanogr* **12**: 343–346
- Lutz KA, Wang W, Zdepski A, Michael TP** (2011) Isolation and analysis of high quality nuclear DNA with reduced organellar DNA for plant genome sequencing and resequencing. *BMC Biotechnol* **11**: 54
- Manoli A, Sturaro A, Trevisan S, Quaggiotti S, Nonis A** (2012) Evaluation of candidate reference genes for qPCR in maize. *J Plant Physiol* **169**: 807–815
- Matsuoka Y, Vigouroux Y, Goodman MM, Sanchez G. J, Buckler E, Doebley J** (2002) A single domestication for maize shown by multilocus microsatellite genotyping. *Proc Natl Acad Sci U S A* **99**: 6080–6084
- Mengutay M, Ceylan Y, Kutman UB, Cakmak I** (2013) Adequate magnesium nutrition mitigates adverse effects of heat stress on maize and wheat. *Plant Soil* **368**: 57–72
- Mühling KH, Läuchli A** (2000) Light-induced pH and K⁺ changes in the apoplast of intact leaves. *Planta* **212**: 9–15
- Munns R** (1993) Physiological processes limiting plant growth in saline soils: some dogmas and hypotheses. *Plant Cell Environ* **16**: 15–24
- Munns R** (2011) Chapter 1 - Plant Adaptations to Salt and Water Stress: Differences and Commonalities. *In* I Turkan, ed, *Adv. Bot. Res.* Academic Press, pp 1–32
- Munns R, Tester M** (2008) Mechanisms of salinity tolerance. *Annu Rev Plant Biol* **59**: 651–681
- Neuhaus C, Geilfus C-M, Zörb C, Mühling KH** (2013) Transcript expression of Mg-chelatase and H⁺-ATPase isogenes in *Vicia faba* leaves as influenced by root and foliar magnesium supply. *Plant Soil* **368**: 41–50
- Niu Y, Jin G, Li X, Tang C, Zhang Y, Liang Y, Yu J** (2015) Phosphorus and magnesium interactively modulate the elongation and directional growth of primary roots in *Arabidopsis thaliana* (L.) Heynh. *J Exp Bot* **66**: 3841–3854
- Okumura M, Inoue S, Kuwata K, Kinoshita T** (2016) Photosynthesis activates plasma membrane H⁺-ATPase via sugar accumulation. *Plant Physiol* **171**: 580–589

- Oury V, Caldeira CF, Prodhomme D, Pichon J-P, Gibon Y, Tardieu F, Turc O** (2016) Is change in ovary carbon status a cause or a consequence of maize ovary abortion in water deficit during flowering? *Plant Physiol* doi: 10.1104/pp.15.01130
- Oury V, Tardieu F, Turc O** (2015) Ovary apical abortion under water deficit is caused by changes in sequential development of ovaries and in silk growth rate in maize. *Plant Physiol* doi: 10.1104/pp.15.00268
- Palmgren MG** (2001) Plant plasma membrane H⁺-ATPases: Powerhouses for nutrient uptake. *Annu Rev Plant Phys* **52**: 817–845
- Palmgren MG** (1991) Regulation of plant plasma membrane H⁺-ATPase activity. *Physiol Plant* **83**: 314–323
- Palmgren MG, Christensen G** (1994) Functional comparisons between plant plasma membrane H⁽⁺⁾-ATPase isoforms expressed in yeast. *J Biol Chem* **269**: 3027–3033
- Pedersen BP, Buch-Pedersen MJ, Preben Morth J, Palmgren MG, Nissen P** (2007) Crystal structure of the plasma membrane proton pump. *Nature* **450**: 1111–1114
- Pitann B, Kranz T, Mühlhng KH** (2009) The apoplastic pH and its significance in adaptation to salinity in maize (*Zea mays* L.): Comparison of fluorescence microscopy and pH-sensitive microelectrodes. *Plant Sci* **176**: 497–504
- Pöpperl G, Oster U, Bios I, Rüdiger W** (1997) Magnesium chelatase of *Hordeum vulgare* L. is not activated by light but inhibited by pheophorbide. *Z Für Naturforschung C* **52**: 144–152
- Porra RJ, Thompson WA, Kriedemann PE** (1989) Determination of accurate extinction coefficients and simultaneous equations for assaying chlorophylls a and b extracted with four different solvents: verification of the concentration of chlorophyll standards by atomic absorption spectroscopy. *Biochim Biophys Acta BBA - Bioenerg* **975**: 384–394
- Qadir M, Noble AD, Schubert S, Thomas RJ, Arslan A** (2006) Sodicy-induced land degradation and its sustainable management: problems and prospects. *Land Degrad Dev* **17**: 661–676
- Rober-Kleber N, Albrechtová JTP, Fleig S, Huck N, Michalke W, Wagner E, Speth V, Neuhaus G, Fischer-Iglesias C** (2003) Plasma membrane H⁺-ATPase is involved in auxin-mediated cell elongation during wheat embryo development. *Plant Physiol* **131**: 1302–1312
- Robinson NE, Bryant JA** (1975) Development of chromatin-bound and soluble DNA polymerase activities during germination of *Pisum sativum* L. *Planta* **127**: 69–75
- Ruan Y-L, Patrick JW, Bouzayen M, Osorio S, Fernie AR** (2012) Molecular regulation of seed and fruit set. *Trends Plant Sci* **17**: 656–665
- Scanlon MJ, Takacs EM** (2009) Kernel Biology. *In* JL Bennetzen, SC Hake, eds, *Handb. Maize Its Biol.* Springer New York, pp 121–143

- Schubert S** (2011) Salt Resistance of Crop Plants: Physiological Characterization of a Multigenic Trait. *In* M J Hawkesford, P Barraclough, eds, *Mol. Physiol. Basis Nutr. Use Effic. Crops*. Wiley-Blackwell, pp 443–455
- Schubert S, Neubert A, Schierholt A, Sümer A, Zörb C** (2009) Development of salt-resistant maize hybrids: The combination of physiological strategies using conventional breeding methods. *Plant Sci* **177**: 196–202
- Sekhon RS, Lin H, Childs KL, Hansey CN, Buell CR, de Leon N, Kaeppler SM** (2011) Genome-wide atlas of transcription during maize development. *Plant J* **66**: 553–563
- Shaul O** (2002) Magnesium transport and function in plants: the tip of the iceberg. *Biometals* **15**: 309–323
- Sondergaard TE, Schulz A, Palmgren MG** (2004) Energization of transport processes in plants. Roles of the plasma membrane H⁺-ATPase. *Plant Physiol* **136**: 2475–2482
- Stout ER, Arens MQ** (1970) DNA polymerase from maize seedlings. *BBA Gene Regul Mech* **213**: 90–100
- Tang A-C, Boyer JS** (2013) Differences in membrane selectivity drive phloem transport to the apoplast from which maize florets develop. *Ann Bot* **111**: 551–562
- Waldron KW, Brett CT** (2008) *Physiology and Biochemistry of Plant Cell Walls*, 2nd ed. Springer
- Wang L, Ruan Y-L** (2013) Regulation of cell division and expansion by sugar and auxin signaling. *Plant Physiol* **4**: 163
- Wang X, Qian X, Stumpf B, Fatima A, Feng K, Schubert S, Hanstein S** (2013) Modulatory ATP binding to the E2 state of maize plasma membrane H⁺-ATPase indicated by the kinetics of vanadate inhibition. *Febs J* **280**: 4793–4806
- Willstätter R, Stoll A** (1913) *Untersuchungen über Chlorophyll: Methoden und Ergebnisse*. Springer-Verlag
- Wrolstad RE, Acree TE, Decker EA, Penner MH, Reid DS, Schwartz SJ, Shoemaker CF, Smith D, Sporns P** (2004) Chlorophylls. *Handb. Food Anal. Chem.* John Wiley & Sons, Inc., pp 153–199
- Yan F, Feuerle R, Schäffer S, Fortmeier H, Schubert S** (1998) Adaptation of active proton pumping and plasmalemma ATPase activity of corn roots to low root medium pH. *Plant Physiol* **117**: 311–319
- Yang L, Arora K, Beard WA, Wilson SH, Schlick T** (2004) Critical role of magnesium ions in DNA polymerase β's closing and active site assembly. *J Am Chem Soc* **126**: 8441–8453
- Yazaki Y, Asukagawa N, Ishikawa Y, Ohta E, Sakata M** (1988) Estimation of cytoplasmic free Mg²⁺ levels and phosphorylation potentials in mung bean root tips by in vivo ³¹P NMR spectroscopy. *Plant Cell Physiol* **29**: 919–924

- Zhao R, Dielen V, Kinet J-M, Boutry M** (2000) Cosuppression of a plasma membrane H⁺-ATPase isoform impairs sucrose translocation, stomatal opening, plant growth, and male fertility. *Plant Cell* **12**: 535–546
- Zinselmeier C, Jeong B-R, Boyer JS** (1999) Starch and the control of kernel number in maize at low water potentials. *Plant Physiol* **121**: 25–36
- Zörb C** (2004) *Biochemische Praktikumsversuche: Einführung in molekularbiologische, proteinbiochemische und quantitative Bestimmungsverfahren in der Biochemie*. Grauer
- Zörb C, Geilfus C-M, Mühling KH, Ludwig-Müller J** (2013) The influence of salt stress on ABA and auxin: concentrations in two maize cultivars differing in salt resistance. *J Plant Physiol* **170**: 220-224
- Zörb C, Mühling KH, Kutschera U, Geilfus C-M** (2015) Salinity stiffens the epidermal cell walls of salt-stressed maize leaves: is the epidermis growth-restricting? *PloS One* **10**: e0118406 doi: 10.1371/journal.pone.0118406
- Zörb C, Noll A, Karl S, Leib K, Yan F, Schubert S** (2005a) Molecular characterization of Na⁺/H⁺ antiporters (*ZmNHX*) of maize (*Zea mays* L.) and their expression under salt stress. *J Plant Physiol* **162**: 55–66
- Zörb C, Stracke B, Tramnitz B, Denter D, Sümer A, Mühling KH, Yan F, Schubert S** (2005b) Does H⁺ pumping by plasmalemma ATPase limit leaf growth of maize (*Zea mays*) during the first phase of salt stress? *J Plant Nutr Soil Sci* **168**: 550–557

Appendix

Table 1: RT-PCR primer pairs for *Zea mays* L. PM H⁺-ATPase and reference genes cullin (CUL) and ubiquitin carrier protein (UBCP)

Primer name	Accession number		Sequence of forward primers	Product size (bp)	Annealing temperature (°C)
<i>MHA 2</i>	GRMZM2G019404	f	CTCTATACCACCAGATACTGCCA	126	55.5
		r	ATTACAACACGCGCACACTC		
<i>MHA 3</i>	GRMZM2G104325	f	ATCGAGACCATCCAGCAGTC	162	55.5
		r	TCATTCATTTCCCGGAACC		
<i>MHA 4</i>	GRMZM2G006894	f	ATCGACACCATCCAGCAGAA	90	55.5
		r	CAAGAACAACAAGGGTGGCA		
<i>MHA 5</i>	GRMZM2G035520	f	ACCATCCAGCAGTCCTACAC	103	55.5
		r	GAAGCCAGCCACCATCAAAT		
<i>MHA 6</i>	GRMZM2G341058	f	ATGGAGTCCGTCGTCGAAGC	80	55.5
		r	CTACACGCATTCACTCACAGG		
<i>CUL</i>		f	GAAGAGCCGCAAAGTTATGG	274	60.0
		r	ATGGTAGAAGTGGACGCACC		
<i>UBCP</i>		f	CAGGTGGGGTATTCTTGGTG	97	60.0
		r	ATGTTCCGGGTGGAAAACCTT		

Figure 1: Dynafit script for model comparison between competitive, noncompetitive, uncompetitive, and Michaelis-Menten kinetics; enzymatic constants and initial values are included.

```

: PH-ATPase at 5 nM Mg, model comparison, confidence intervals ;
No discrimination between ATP species F .....

[task]
data = velocities
task = fit
model = competitive ?

[mechanism]
Mg + ATP <==> S          : kang kdmg
E + S <==> E.S          : kas kds
E.S <==> E + P          : kr
E + ATP <==> E.ATP       : ka kd

[constants]
kang = 1, kdmg = 28.18      ; Kd(MgATP) = 28.18 uM [IUPAC, 1991]
kas = 10, kds = 1200 ??    ; Km = 120 uM ?
kr = 58 ??                 ; kr = .0058/[ET] = 58 / s ?
ka = 10, kd = 3000 ??     ; Kd = 300 uM ?

[responses]
P = 1

[concentrations]
E = 0.0001, Mg = 5000      ; [ET] = 10 ug/L = 100 pM

[progress]
delay = 3 ; 3 second mixing delay time

[veloc]
directory ./examples
extension txt
variable ATP
file ControlNSmMg

[output]
directory ./ControlNSmMgallies

[task]
data = velocities
task = fit
model = uncompetitive ?

[mechanism]
Mg + ATP <==> S          : kang kdmg
E + S <==> E.S          : kas kds
E.S <==> E + P          : kr
E.S + ATP <==> E.S.ATP   : ka2 kd2

[constants]
kang = 1, kdmg = 28.18      ; Kd(MgATP) = 28.18 uM (IUPAC, 1991)
kas = 10, kds = 1200 ??    ; Km = 120 uM ?
kr = 58 ??                 ; kr = 0.058/[ET] = 58 / s ?
ka2 = 10, kd2 = 3000 ??

[task]
data = velocities
task = fit
model = noncompetitive ?

[mechanism]
Mg + ATP <==> S          : kang kdmg
E + S <==> E.S          : kas kds
E.S <==> E + P          : kr
E + ATP <==> E.ATP       : ka kd
E.S + ATP <==> E.S.ATP   : ka kd
E.ATP + S <==> E.S.ATP   : kas kds

[constants]
kang = 1, kdmg = 28.18      ; Kd(MgATP) = 28.18 uM (IUPAC, 1991)
kas = 10, kds = 1200 ??    ; Km = 120 uM ?
kr = 58 ??                 ; kr = 0.058/[ET] = 58 / s ?
ka = 10, kd = 3000 ??     ; Kd = 300 uM ?

[task]
data = velocities
task = fit
model = Michaelis-Menten ?

[mechanism]
Mg + ATP <==> S          : kang kdmg
E + S <==> E.S          : kas kds
E.S <==> E + P          : kr

[constants]
kang = 1, kdmg = 28.18      ; Kd(MgATP) = 28.18 uM [IUPAC, 1991]
kas = 10, kds = 1200 ??    ; Km = 120 uM ?
kr = 58 ??                 ; kr = .0058/[ET] = 58 / s ?

[end]

```

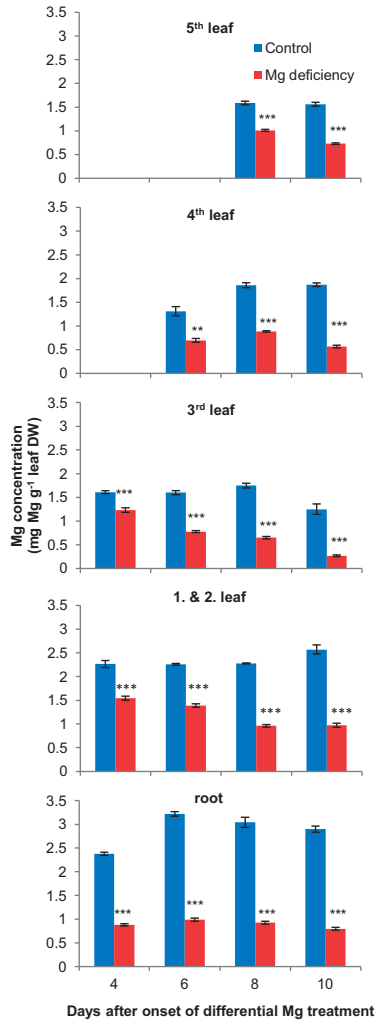


Figure 2: Effect of Mg nutrition on Mg concentration of leaves and roots of maize. Control (blue) nutrient solution with 500 μ M Mg, Mg deficiency (red) with 25 μ M Mg; means ($n = 4$) \pm SE. Significant differences at *** $P = 0.1\%$ between control and the Mg-deficiency treatment.

Acknowledgment

I am extremely grateful to Prof. Dr. Sven Schubert for giving me various opportunities to grow as a scientist and as a human being at the institute and enabling me to write this thesis. His guidance, close supervision and support pushed the doors of science wide open for me. I thank him for taking so much time to patiently checking manuscripts and for always having an open ear. Thanks!

I also thank Prof. Dr. Sylvia Schnell for agreeing to be my co-supervisor. I am very grateful for her support especially in the early time of my PhD. Prof. Schnell and Dr. Stefan Ratering helped me a great deal in establishing a concept for the establishment of a PGPB-plant interaction system. Thank you very much for staying interested and supportive to me and my PhD project after the microbiological aspects of my topic did not work out as planned.

I thank Prof. Michael Palmgren, University of Copenhagen for providing information and interpretation about the 3D structure of the PM H⁺-ATPase.

Thank you to Prof. Dr. Diedrich Steffens for introducing me to plant nutrition and the institute at the beginning of my master thesis. I am grateful for a lot of helpful discussion about experimental designs, various aspects about plant nutrition and all aspects of life in general.

Special thanks to Franziska Faust and Johanna Krippner for your great help at numerous occasions over the last years. You are both incredible smart women with a great future ahead of you!

I thank Dr. Birgit Hütsch for being a great colleague and a wonderful partner in the project: “Kernel development of maize.”

Special thanks to our good souls of the institute Christina Plachta and her administrative counterpart Sigrid Beckermann. Your ability to manage the lab and the office as well as your kindness helped a very great deal in the last years.

Also special thanks to Roland Pfanschilling who helped me a lot at the beginning of my master and PhD thesis with all aspects of agriculture-chemical lab work. The same goes to Christa Lein who introduced me to various biochemical and protein-biochemical methods. I am also extremely grateful to our gardeners Corinna Alles-Becker, Helga Tripp and Lutz Wilming for taking excellent care of all my plants during various experiments over the years. Claudia Weimer and Edeltraud Roediger for their help in general and especially with a lot of mind-numbing tasks which they always carried out swiftly and accurately. Thanks are also due to Anita Langer for her great assistance in various fields in the lab. Thanks to Elke Kauffeld for her aid in the determination of cation concentrations.

I am also grateful to Philipp Eitenmüller, Daniel Steckenmesser and Alexandra Wening for their help in various aspects of every day work and life.

Thanks are due to Ole Bartz, Thomas Klintzsch, Leon Lingenberg and Michael Schlüter for keeping up my spirits on and of work during the last years.

I am very grateful to the whole Institute of Soil Science. There I walked my first steps into the world of science. Special thanks to Prof. Dr. Felix-Henningsen, Prof. Dr. Rolf Düring, Sylvie Drahorad, Leo Böhm, Hülya Kaplan, Vincent Felde and Thomas Hanauer as well as Marianne Grünhäuser, Elke Müller and Elke Schneidenwind.

Special thanks to my parents, who always supported me during my nearly 10 years of university education in every possible aspect. You always encouraged me to find my own way in life. I am tremendously grateful for that.

Last, but not least thank you very much to my partner in love and crime Carsten, who has always been there for me during the last years.

Declaration

“I declare that the dissertation here submitted is entirely my own work, written without any illegitimate help by any third party and solely with materials as indicated in the dissertation. I have indicated in the text where I have used texts from already published sources, either word for word or in substance, and where I have made statements based on oral information given to me. At all times during the investigations carried out by me and described in the dissertation, I have followed the principles of good scientific practice as defined in the “Statutes of the Justus Liebig University Giessen for the Safeguarding of Good Scientific Practice.”

Giessen, September 05, 2016

Stephan Jung

**Der Lebenslauf wurde aus der elektronischen
Version der Arbeit entfernt.**

**The curriculum vitae was removed from the
electronic version of the paper.**

Publications

Peer-reviewed publications:

Hanauer T, Jung S, Felix-Henningsen P, Schnell S, Steffens D (2012) Suitability of inorganic and organic amendments for *in situ* immobilization of Cd, Cu, and Zn in a strongly contaminated Kastanozem of the Mashavera valley, SE Georgia. I. Effect of amendments on metal mobility and microbial activity in soil. *Journal of Plant Nutrition and Soil Science* **175**: 708–720

Hütsch BW, Jung S, Schubert S (2015) Comparison of salt and drought-stress effect on maize growth and yield formation with regard to acid invertase activity in the kernels. *Journal of Agronomy and Crop Science* **201**: 353–367

Suarez C, Cardinale M, Ratering S, Steffens D, Jung S, Montoya AMZ, Geissler-Plaum R, Schnell S (2015) Plant growth-promoting effect of *Hartmannibacter diazotrophicus* on summer barley (*Hordeum vulgare* L.) under salt stress. *Applied Soil Ecology* **95**: 23–30

Jung S, Krippner J, Schubert S (2016) Is the photometric method using acetone extracts to determine chlorophyll concentrations applicable to Mg-deficient plants? *Journal of Plant Nutrition and Soil Science* **179**: 439–442

Jung S, Faust F, Schubert S (2016) Reduced apoplastic acidification caused by altered PM H⁺-ATPase activity is responsible for early growth reduction of maize under Mg deficiency. *Environmental and Experimental Botany*, submitted

Jung S, Hütsch B, Schubert S (2016) Salt stress reduces kernel number of corn by inhibiting plasma membrane H⁺-ATPase activity. *Plant Physiology*, submitted

Talks and non-reviewed publications:

Talks:

Jung S, Hanauer T, Schubert S, Felix-Henningsen P, Steffens D: *In situ*-remediation of a heavy metal-contaminated Kastanozem by various soil amendments. 15th ICHMET (International Conference on Heavy Metals in the Environment, 19.-23.09.2010) Gdańsk (Danzig), Poland.

Jung S, Hanauer T, Schubert S, Felix-Henningsen P, Wissemeier A, Steffens D: Melioration schwermetallbelasteter Böden und Substrate durch Bodenadditive. DGG (Deutsche Gartenbauwissenschaftliche Gesellschaft) Jahrestagung 2011 (23.-26.02. 2011), Hannover

Jung S, Ander C, Schubert S: Effect of drought and salt stress on kernel setting of maize. Congress "Plant Growth, Nutrition and Environment Interactions", Vienna, Austria, February 18.-21. 2012

Jung S, Hanauer T, Schubert S, Felix-Henningsen P, Steffens D: Testing of inorganic and organic amendments for *in situ* stabilization of Cd, Cu & Zn in a strongly contaminated Kastanozem. Congress "Eurosoil 2012", Bari, Italy, 02.-06.07.2012

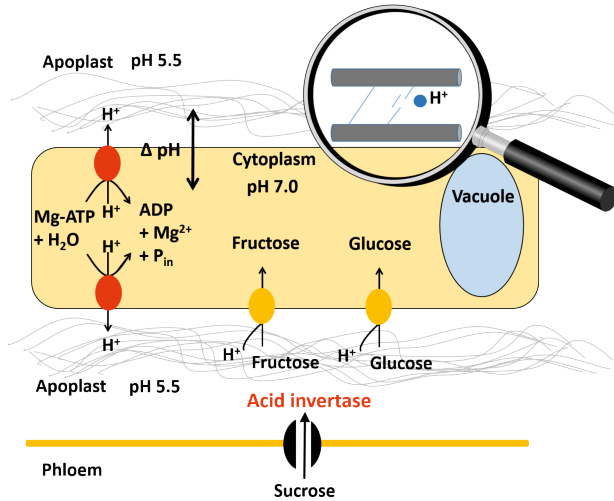
Posters:

Jung S, Ander C, Schubert S: Effect of drought and salt stress on growth and grain yield of different maize genotypes. Jahrestagung der Deutschen Gesellschaft für Pflanzenernährung, Bonn, 05.09.-07.09.2012.

Jung S, Alifkina M, Schubert S: Effect of *Bacillus amyloliquefaciens* on P acquisition of maize. Jahrestagung der Deutschen Gesellschaft für Pflanzenernährung, Freising. 09.05.-10.05.2013.

Jung S, Hanauer T, Schubert S, Felix-Henningsen P, Steffens D: Suitability of inorganic and organic amendments for *in situ* immobilization of Cd, Cu, and Zn in a strongly contaminated Kastanozem. "International Plant Nutrition Colloquium" (IPNC) (Istanbul, Turkey). 19.08.-22.08.2013

Jung S, Hütsch B, Schubert S: Effect of drought and salt stress on growth and grain yield of different maize genotypes. Interdrought IV, (Perth, Australia) 02.09.-06.09.2013



édition scientifique
VVB LAUFERSWEILER VERLAG

VVB LAUFERSWEILER VERLAG
STAUFENBERGRING 15
D-35396 GIESSEN

Tel: 0641-5599888 Fax: -5599890
redaktion@doktorverlag.de
www.doktorverlag.de

ISBN: 978-3-8359-6538-6

